

Fall 2011

YIG-sphere-based phase shifter for X-band phased array applications

Donald C. Benson
San Jose State University

Follow this and additional works at: https://scholarworks.sjsu.edu/etd_theses

Recommended Citation

Benson, Donald C., "YIG-sphere-based phase shifter for X-band phased array applications" (2011). *Master's Theses*. 4083.

DOI: <https://doi.org/10.31979/etd.p4je-rvaz>

https://scholarworks.sjsu.edu/etd_theses/4083

This Thesis is brought to you for free and open access by the Master's Theses and Graduate Research at SJSU ScholarWorks. It has been accepted for inclusion in Master's Theses by an authorized administrator of SJSU ScholarWorks. For more information, please contact scholarworks@sjsu.edu.

YIG-SPHERE-BASED PHASE-SHIFTER FOR X-BAND PHASED
ARRAY APPLICATIONS

A Thesis

Presented to

The Faculty of the Department of Electrical Engineering

San José State University

In Partial Fulfillment

of the Requirements for the Degree

Master of Science

by

Donald C. Benson

December 2011

© 2011

Donald C. Benson

ALL RIGHTS RESERVED

The Designated Thesis Committee Approves the Thesis Titled

**YIG-SPHERE-BASED PHASE-SHIFTER FOR X-BAND PHASED
ARRAY APPLICATIONS**

by

Donald C. Benson

APPROVED FOR THE DEPARTMENT OF ELECTRICAL ENGINEERING

SAN JOSÉ STATE UNIVERSITY

December 2011

Dr. Sotoudeh Hamedi-Hagh

Department of Electrical Engineering

Dr. Masoud Mostafavi

Department of Electrical Engineering

Dr. Raymond Kwok

Department of Physics

ABSTRACT

YIG-SPHERE-BASED PHASE SHIFTER FOR X-BAND PHASED ARRAY APPLICATIONS

By Donald C. Benson

A novel technique for effecting phase shift of X-band signals has been developed and analyzed for use with quadrature amplitude modulation (QAM) of signals in a phased array application, and the impact of this phase shifter on error vector magnitude (EVM) has been quantified. A commercially available filter consisting of yttrium iron garnet (YIG) spheres was characterized by means of a network analyzer. The gain and phase response was measured across a 25 MHz frequency band centered at 10 GHz, while the filter was tuned in frequency steps such that a 360° range of phase shifts was achieved. The S-parameters from these measurements were integrated with Matlab representations of QAM-16 modulation, demodulation, and phased array antennas to model a complete radio system. The EVM caused by non-ideal gain and phase response of the YIG filter was determined for various beam angles and data patterns.

It was found that a YIG filter does provide stable phase shift suitable for phased array applications, with acceptable attenuation so long as the frequency being transmitted remains within the filter's pass band. The particular filter analyzed did not contain sufficient stages to maintain 3 dB flatness across the required 360° tuning range, but performed satisfactorily for a limited range of beam orientation. The capability to provide continuously variable phase shift offered by the YIG filter was found to not offer significant advantage over the discrete steps produced by switched delay lines.

Table of Contents

I.	Introduction	1
A.	Background.....	1
B.	Related research.....	1
C.	Selection of YIG sphere technology.....	3
II.	Hypothesis.....	8
III.	Partition between hardware and mathematical simulation.....	9
IV.	Implementation of YIG phase shifter.....	11
D.	Design of a custom filter	11
E.	Selection of a commercial filter	13
F.	Characterization of filter.....	14
V.	The behavior of phased arrays	22
VI.	Simulation of radiation pattern.....	24
VII.	Simulation of modulation/demodulation and error vector magnitude	28
G.	Baseline model of digital radio with ideal channel	28
H.	Three-bit phase shifter for beam forming.....	39
I.	Ideal Butterworth filter phase shifter for beam forming	40
J.	Measured YIG filter phase shifter for beam forming.....	44

K.	YIG filter phase shifter operated within -3 dB bandwidth	46
L.	Swept beam angle using YIG filter phase shifter	48
VIII.	Issues identified in phased array systems	50
IX.	Potential pitfalls of characterization and analysis approach	52
X.	On implementing an actual system	54
XI.	Conclusion.....	55
APPENDIX A.	Matlab code	56
A.	Radiation pattern	56
B.	Antenna pattern	60
C.	Constructive and destructive interference	61
D.	Phase shifter.....	63
E.	Digital radio model and EVM calculation.....	66
F.	Idealized Butterworth beam former.....	84
G.	Idealized Butterworth phase shifter	86
H.	Recovery synchronization	89
I.	YIG beam former	93
J.	YIG phase shifter.....	96
K.	Swept beam angle.....	98

L.	Read S-parameter files and store in array.....	99
M.	Read and plot filter S-parameter across entire passband.....	110
APPENDIX B.	Data files.....	120
A.	YIG S-parameter	120
References.....		128

List of Figures

Figure 1.	Schematic representation of YIG bandpass filter	3
Figure 2.	Original concept of bi-directional system	5
Figure 3.	Transformation of impedance through stages of a filter	11
Figure 4.	YIG filter	13
Figure 5.	S-parameter test setup	15
Figure 6.	2 - 20 GHz response of YIG filter	17
Figure 7.	Measured gain and phase of YIG filter across the pass band	18
Figure 8.	Measured gain and phase of YIG filter across frequency band of radio	20
Figure 9.	Phase shift vs. beam angle	22
Figure 10.	Radiation pattern with ideal phase shifters	25
Figure 11.	Radiation pattern with 3-bit phase shifters	26
Figure 12.	Radiation pattern with YIG phase shifters	26
Figure 13.	Constellation and I/Q modulation of [56A9401237BFEDC8]	33
Figure 14.	QAM-16 modulation and frequency content of [56A9401237BFEDC8]	34
Figure 15.	Recovered constellation, I & Q, and error for [56A9401237BFEDC8]	36
Figure 16.	Constellation and I/Q modulation of [0F4B87C3D2E1A569]	37
Figure 17.	QAM-16 modulation and frequency content of [0F4B87C3D2E1A569]	38
Figure 18.	Recovered constellation, I & Q, and error for [0F4B87C3D2E1A569]	39
Figure 19.	Recovered constellation, I & Q, and error, 3-bit phase shifter	40

Figure 20. Butterworth bandpass filter tuned around 10 GHz to provide phase shift	41
Figure 21. Recovered constellation, I & Q, and error, Butterworth phase shifter	43
Figure 22. Recovered constellation and delta error YIG vs. baseline	45
Figure 23. Recovered constellation and delta error YIG vs. baseline for small angle	47
Figure 24. EVM variation as beam swept from 0° to $+90^{\circ}$ by YIG phase shifter	49

List of Tables

TABLE I. I and Q encoding of symbols

30

I. INTRODUCTION

A. Background

Passive technologies used to provide continuously variable phase shift for lower frequencies up to a few gigahertz, such as LC filters tuned with varactor diodes, do not meet the needs of operation in the 10 GHz X-band region. Alternatives such as switched delay lines offer only discrete steps in delay, while active monolithic microwave integrated circuit (MMIC) devices used to generate signals for each antenna element add complexity and cost. Custom thin-film yttrium iron garnet (YIG) phase shifters have also been an area of research. YIG filters and resonators such as those offered by Microlambda Wireless [1] have been used for other applications in communication and test equipment.

B. Related research

Technologies used to provide continuously variable phase shift for lower frequencies up to a few gigahertz do not function at X-band frequencies (8.2 to 12.4 GHz). YIG thin films and YIG slabs have been used to provide adjustable propagation delays for signals carried by microstrip or stripline transmission lines operating at such frequencies. They have also been used to provide delayed coupling between parallel transmission lines placed over the YIG material. Demidov et al. [2] described the use of yttrium-iron-garnet (YIG) films grown on substrates of suitable lattice dimensions, especially gadolinium-gallium-garnet (GGG), as a tunable magnetic medium for phase shifters. With this material placed over microstrips, the propagation delay of electromagnetic waves could be varied with an externally applied magnetic field. How et al. [3] noted that operating

frequency had to be well away from the resonant frequency the YIG was tuned to or the losses would be high. That tendency to dissipate energy at resonance is similar to having a high frequency decoupling capacitor (a deliberately fabricated capacitor in series with parasitic inductance), which serves to absorb energy at its resonant frequency. The same behavior can also be obtained with a discrete inductor and capacitor. Either way, this circuit may be used to reduce noise such as harmonics from a digital system that affects radio reception. However, such attenuation is undesirable when shifting the phase of a signal.

Tatarenko et al. [4] described phase shifters using the characteristic of YIG that it rotates the orientation of a magnetic field at its resonant frequency. The design described took advantage of this behavior with two orthogonal microstrips placed over a YIG disc. YIG-tuned filters utilizing the same behavior, which permits precision control based on a tunable resonant frequency, are similarly constructed by placing two orthogonal loops of wire around a YIG sphere (see Fig. 1).

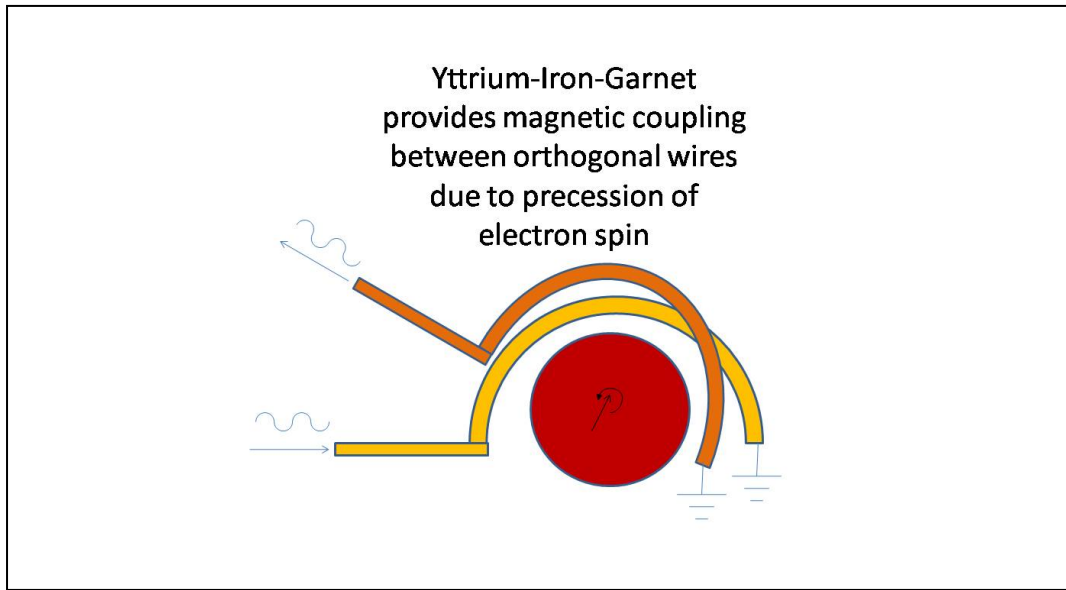


Figure 1. Schematic representation of YIG bandpass filter

In this configuration the YIG implements a transformer with behavior similar to an LC bandpass filter with $Q=1000$. At the resonant frequency, rather than dissipating the input energy, the circuit couples it effectively to the output. The use of a YIG disc as a phase shifter is the closest to the work described in this thesis, as there are no known reports of YIG spheres used as phase shifters.

Finally, Foster et al. [5] described using water-cooled slabs of YIG in a waveguide to provide adjustable timing of a 2MW signal used in a particle accelerator.

C. Selection of YIG sphere technology

Phase shifters based on YIG spheres were selected for study based on apparent advantages over other technologies.

Compared to coaxial or microstrip delay lines that are switched by microwave relays, producing discrete steps in phase shift (for instance, dividing the $\pm 180^\circ$ range into 45° or 22.5° increments based on a 3-bit or 4-bit index), the YIG phase shifter offers a continuously variable response. This allows higher antenna gain due to the narrower, more highly directional beam. Furthermore, switching of relays requires milliseconds, whereas the continuous adjustment of YIG means all antenna elements would continuously contribute to beam forming, except during the time when they retrace from $+180^\circ$ to -180° .

Signals from separate antenna elements can be phase shifted through the YIG phase shifters without active microwave devices for each antenna element. Finally, unlike thin-film YIG phase shifters which are a current subject of research, use of commercially available YIG spheres avoid custom device development and fabrication. For higher volume applications, the development of custom processes may be warranted by lower unit costs. The application being considered, however, might require a single 15×15 element antenna array. Assembling phase shifters using current hybrid substrate fabrication and assembly techniques such as ribbon bonding can result in a shorter schedule and reduced cost.

The concept of a phased array system for full duplex communication is presented in Fig. 2.

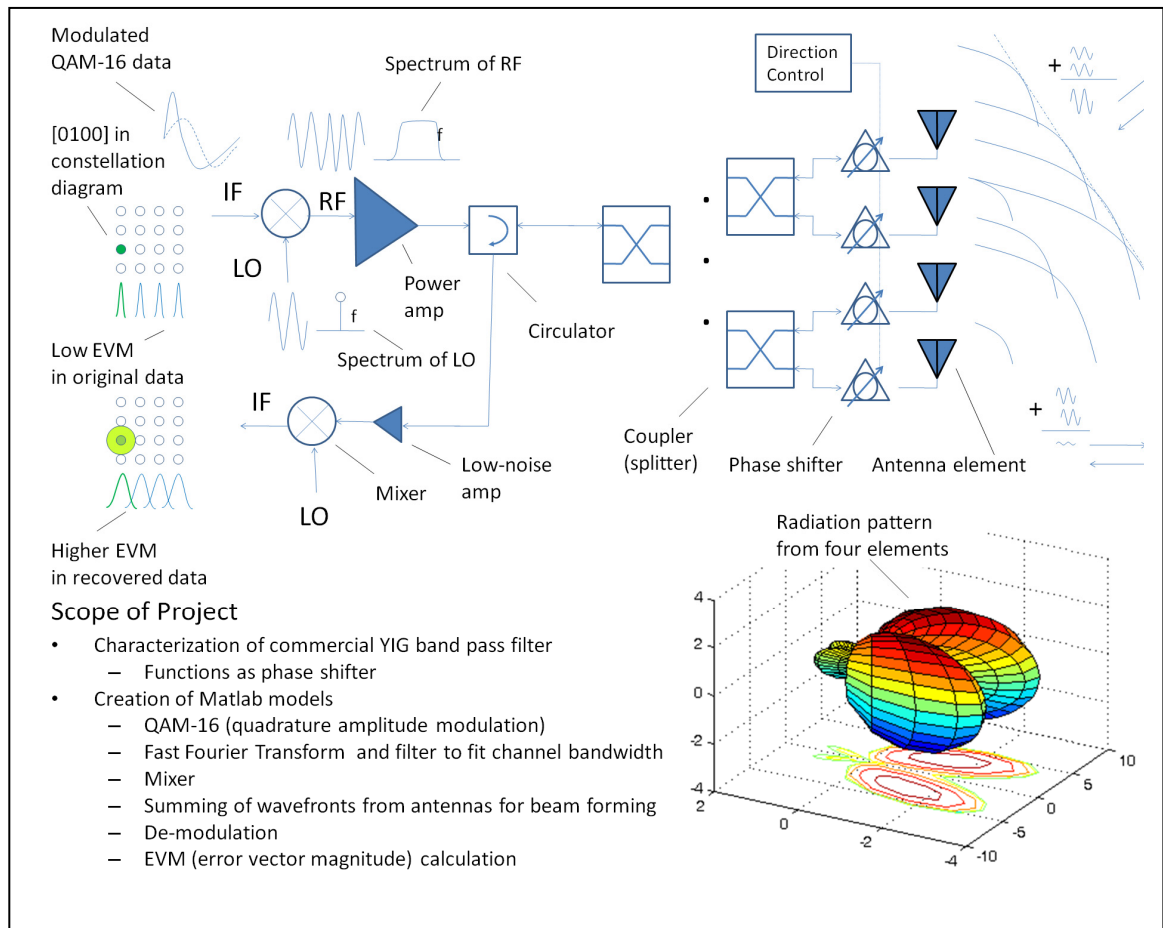


Figure 2. Original concept of bi-directional system

A bit stream of hexadecimal symbols (0 through F) is modulated as QAM-16 constellations, with two bits selecting a row and two bits selecting a column in the constellation. The X-axis, referred to as I , modulates the amplitude of a sinusoidal signal while the Y-axis, referred to as Q , modulates the amplitude of another sinusoidal signal that is 90° out of phase with the first one. When these two amplitude-modulated signals are summed, the result is an amplitude and phase-modulated signal. Although this signal has a single frequency with constant amplitude and phase, the transition between

modulated symbols introduces other frequency components of varying amplitudes. The frequency envelope shown represents what might be present in a long string of symbols (after filtering to remove the infinite number of higher harmonics generated by the abrupt change between symbols). This signal, referred to as intermediate frequency (IF), is then multiplied with the signal from a local oscillator (LO) by means of a non-linear component called a mixer. The resultant frequency spectrum includes all frequencies coming from (1) where n and m are all positive integers.

$$n \times LO \pm m \times IF \quad (1)$$

After filtering to remove the undesired images, the RF signal contains the transmitted information centered about the carrier frequency, which is the sum of LO and IF frequencies.

After amplification, the RF signal is split and sent through phase shifters to the antenna elements. Each phase shifter is directed to introduce a delay or phase shift, such that the transmitted signal will be in phase with signals from other antenna elements when they are the same distance from the desired target.

For the receive path, after phase shifting the signals that arrived at the antenna elements at different times so they constructively interfere (i.e., add linearly because they are in phase), the signals are summed and directed to the demodulation circuitry. The received RF is multiplied by LO and the desired IF from (2) is filtered out.

$$RF - LO = IF \quad (2)$$

The IF is then sampled and multiplied by two sinusoids 90° out of phase with each other (and suitably synchronized in phase with the IF signal) to recover I and Q values. Due to errors in the system such as undesired frequency-dependent attenuation or phase shift, these values will not be precisely the ones sent. The nearest allowable value is selected, and so long as the error is less than 50% of the difference between levels representing adjacent points in the constellation, the data can be recovered without error. The deviation from ideal values is Error Vector Magnitude, a key metric of channel quality.

As originally conceived, the YIG filter would be used as a phase shifter in a bi-directional digital radio system, with only passive elements (the phase shifters and splitter/combiners) between the power amplifier (PA)/low noise amplifier (LNA) and the antenna, as shown in Fig. 2. The idea for this architecture was based on some literature that suggested each sphere could transfer as much as 2W of power. However, specifications for some commercially available YIG band pass filters showed only 10 mW of power handling capability [1]. A commercially built filter was subjected to a power sweep from -50 dBm to +20 dBm (100 mW is the maximum output available from the Agilent E8364B VNA) at 10.0 GHz, and no compression was observed. Further testing with an external amplifier would be required to measure the response at higher power. If not able to handle at least 1W, without the addition of power amplifiers for each antenna element, this technology is appropriate only for receiver (but not transmitter) applications, such as gathering telemetry data.

II. HYPOTHESIS

Several technologies are currently used for phase shifters. One type is based on varactor diodes, which provide a continuously variable capacitance when bias voltage is changed. Varactor phase shifters are capable of operating up to the low gigahertz frequency range but are not suitable for X-band. Another type that is used for X-band has relays to switch between fixed delay lines of different lengths. Switched delay line phase shifters provide very flat gain response but offer adjustment only in discrete steps and carry no power during the switching transition. A third type currently used for phased arrays at X-band frequencies and higher is based on monolithic microwave-integrated circuit (MMIC) technology. MMIC phase shifters vary the amplitude of sine and cosine signals to provide a continuously adjustable phase shift.

A band-pass filter based on YIG spheres will provide precise phase shift, with acceptable variation in attenuation, resulting in higher gain of a phased array antenna system operating at X-band microwave frequencies compared to discrete delay lines. The continuously variable response will permit rapid sweeping of beam direction without loss of power to antenna elements due to switching. The ability to provide phase-shift without active microwave devices for each antenna will permit a lower-cost implementation.

III. PARTITION BETWEEN HARDWARE AND MATHEMATICAL SIMULATION

In order to show the impact of YIG phase shifters on total system performance, a physical YIG phase shifter was characterized on a network analyzer and the rest of the communication system was modeled as idealized elements in Matlab. A typical system would use a two-dimensional antenna array to direct the beam in elevation as well as azimuth. To simplify bookkeeping within the simulation and graphical representation of radiation patterns a one-dimensional array was modeled. A real system would use patch antennas because they are appropriate to support beam-forming in two dimensions. The idealized Hertzian dipole was used for this study. Three-dimensional equations for the Hertzian dipole were used, and the three-dimensional radiation pattern was reviewed graphically for validity.

Initially an idealized phase shifter was modeled. This was compared to simulation of an ideal Butterworth bandpass filter (as representative of an ideal YIG filter), a simulation of 3-bit (45° increment) phase shifters consisting of coaxial cables (a typical phase shifter used in microwave applications), and finally captured S-parameters from the YIG phase shifter.

To make the Butterworth filter tunable for phase shift, it was parameterized such that values were computed according to center frequency, and the center frequency was selected based on desired phase shift. Similarly, an array of measured YIG phase shifter S-parameters generated at various magnetic field intensities was used to generate the response for each element. Initially linear interpolation was considered, but 10°

increments were found to be close enough to ideal, so the measured S-parameter with phase shift closest to the desired value was used without interpolation.

IV. IMPLEMENTATION OF YIG PHASE SHIFTER

D. Design of a custom filter

The original plan was to fabricate a filter with the desired characteristics. A phase shifter capable of 360° phase shift is necessary to support even limited pointing angles (less than 180°) with a large number of elements spanning a distance much larger than one wavelength. Review of commercially available YIG bandpass filters showed that a filter consisting of four YIG spheres was required to obtain this phase shift. The Butterworth filter approximation provides maximally flat pass-band response with a relatively linear phase shift, so this implementation was targeted. A study of the Butterworth filter reveals that each section is resonant at the same frequency, but component parameters vary such that the input impedance of each stage is matched to the output impedance of the previous stage (see representative lowpass Fig. 3).

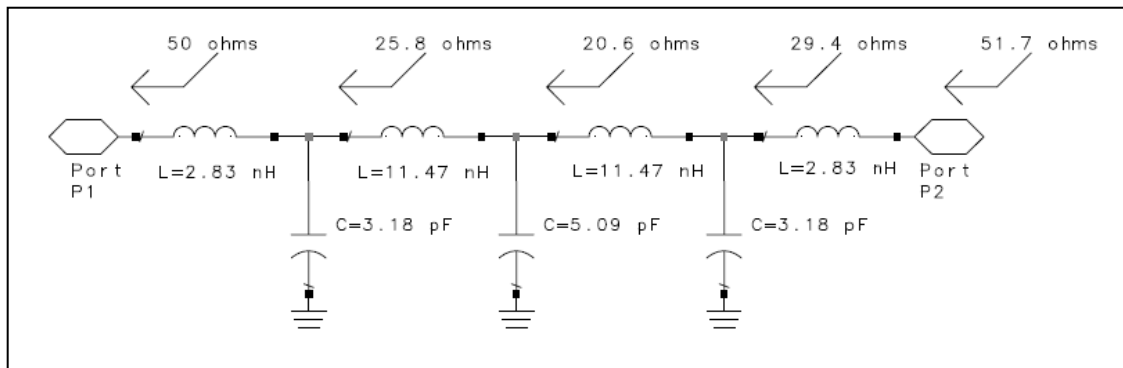


Figure 3. Transformation of impedance through stages of a filter

Without equations or simulation models in Agilent ADS representing YIG's behavior of capturing magnetic energy and coupling it into an orthogonal wire, it would be

necessary to devise a method to appropriately determine dimensions for a prototype. Although this unique behavior was not available as a model parameter in ADS, magnetic permeability is a standard material parameter. The approach that would be taken is to select dimensions of the wire loop such that with the sphere inside, impedance of 50Ω would be maintained. The orthogonal wire loop dimensions would be set to achieve the desired output impedance for the first stage, and dimensions of other stages would be determined in a similar manner to maintain impedance match between stages.

The physical implementation initially conceived was to design a hybrid substrate with appropriate dielectric such as Teflon. Various low-temperature co-fired ceramics (LTCC) would also be appropriate, but prototype techniques and shrinkage issues make these more difficult than etching of a double-sided laminate. Interconnect between each stage would be designed to match the targeted impedance. Metalization supporting gold wirebonding would be required. Loops were to be formed with a ribbon bonder, providing interconnect with a wide cross-section for low resistive losses. SMA connectors would be soldered to the substrate.

Further investigation revealed that tuning of a multi-stage YIG filter is a relatively involved process. Resonant frequency and input and output impedances of each stage must be correct, as with any multi-stage filter. However, the degrees of freedom to be adjusted for a YIG filter are not just loop area and sphere location; the spheres themselves must be binned for desired characteristics [6]. This made such an implementation beyond

the scope of this project. Accordingly, a commercially available YIG filter was characterized.

E. Selection of a commercial filter

Due to the difficulty of fabricating a YIG filter with sufficient performance, a commercially available YIG filter from Yig Tek was obtained, model number 183-43 (see Fig. 4).

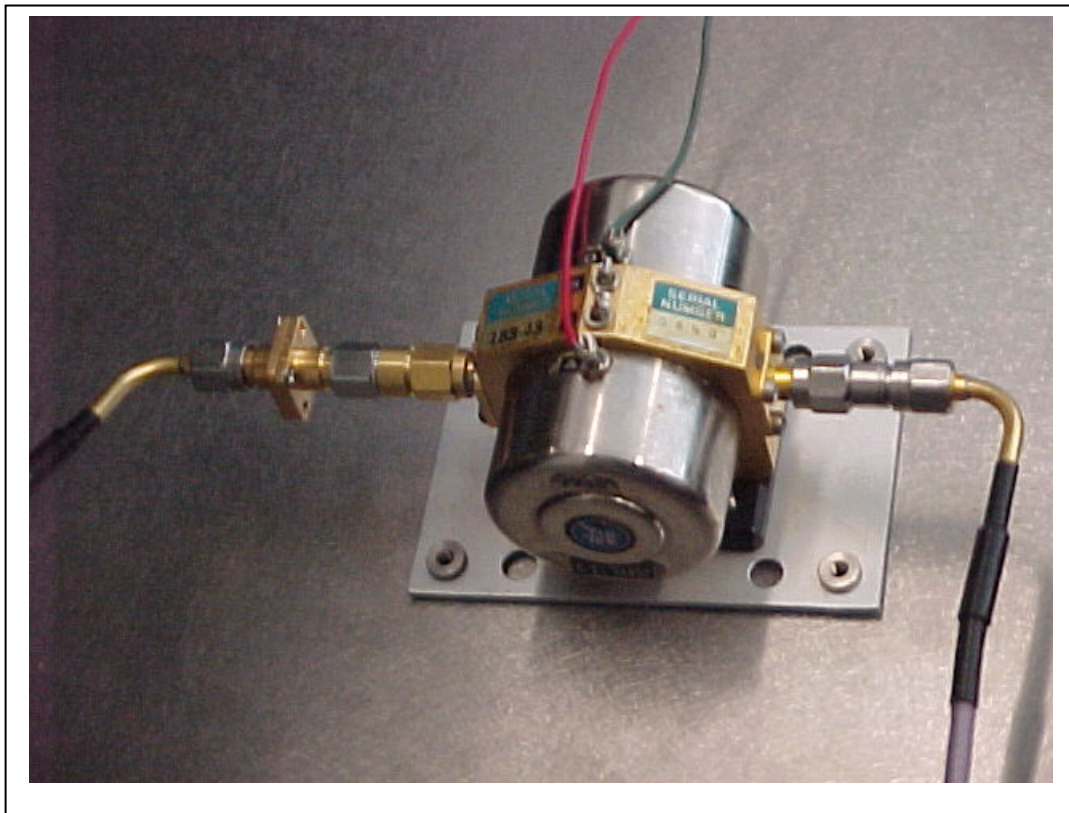


Figure 4. YIG filter

F. Characterization of filter

For actual usage it is necessary to stabilize the temperature of the YIG sphere. Variations in ambient temperature, and variations in self-heating depending on RF power, would cause a drift in response. By heating the YIG sphere to a regulated temperature RF performance can be measured and recorded as calibration data correlating tuning current with frequency.

According to Bryant et al. [7], “Heating to 105 C +/- 5 gives approximately seven fold reduction in changes due to temperature variation.” This is one of the techniques that gives YIG sphere based oscillators the frequency stability required for use as a time base in microwave test equipment such as Vector Network Analyzers (VNA) and Spectrum Analyzers. The commercially available YIG filter which was characterized has an internally regulated heater for this purpose. With variation of temperature reduced, only regulation of current used to generate the magnetic field is necessary to set resonant frequency, and the YIG filter operates with stable phase shift. For the purpose of this work, the YIG filter was permitted to stabilize at operating temperature and measurements were performed with steady state (or repeatedly swept) RF power, so the heater was not required.

Characterization was performed with an Agilent E8364B 50 GHz Vector Network Analyzer (VNA), connected to the YIG filter with Gore cables and 2.4mm to SMA adapters (see Fig. 5).

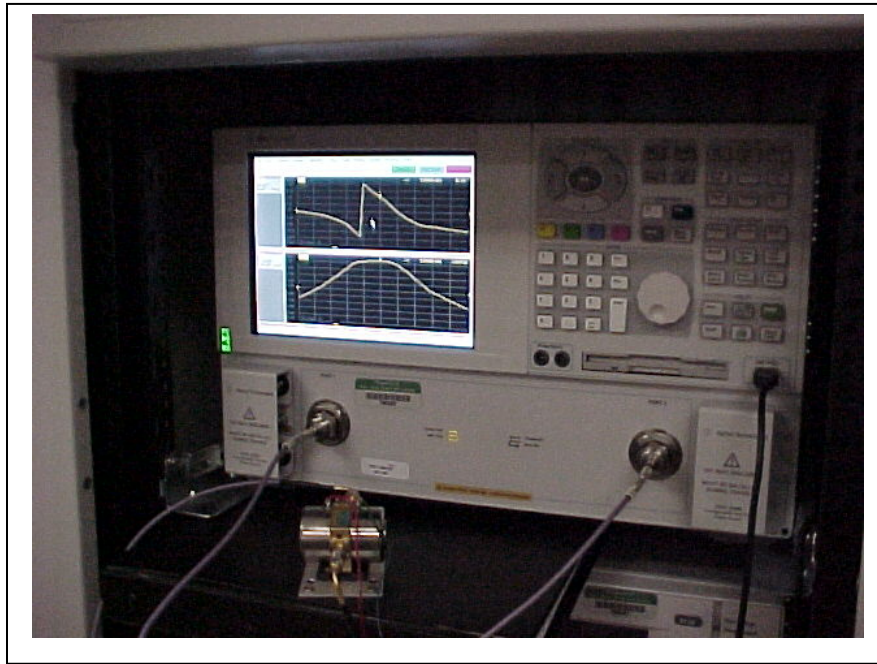


Figure 5. S-parameter test setup

Bias current for the electromagnet was provided by two Agilent E3630A +6V, +/-20V power supplies. A regulated current source should be used, but none was readily available, so a series resistor was used instead to set a current from the voltage source. To achieve sufficient resolution to allow tuning of the filter phase shift in 10° increments ($\pm 3^\circ$), the supplies were connected in series to provide 46V. The YIG filter tuning coil has nominal 6Ω DC resistance, and two, 50Ω 10W resistors were connected in series. Resolution of the control for the power supply output voltage was the limiting factor in adjusting frequency and phase shift of the filter. Current ranging from 380 mA to 420 mA spanned the desired tuning range, but only a slight nudge to the control knob changed phase by more than 10° . A circuit utilizing a 10-turn potentiometer or digital control

would have been easier to use. At any given setting, however, the response was stable; phase jitter was only 0.4° and gain jitter was only 0.05 dB with the network analyzer's averaging function turned off. Averaging was turned on for calibration and data gathering. The addition of a $2.5\text{ K}\Omega$ potentiometer in parallel with the YIG filter's tuning coil allowed adjusting the response with sufficient resolution to easily select the desired 10° increments.

An attempt was made to determine power handling of the filter by sweeping power from -50 dBm to +20 dBm (100 mW, which is the maximum VNA output), but no gain compression was observed. An external power amplifier (PA) would be required to find the capability of this filter.

Frequency sweeps were taken at 0 dBm RF power and various magnetic field strengths producing a phase shift (at 10 GHz) of -180° to $+180^\circ$ in 10° steps; the data from these 36 frequency sweeps were stored as S-parameter files. Frequency steps are typically linear or logarithmic when generated by test equipment, unlike electromagnetic field solvers that may increase resolution depending on simulated response. If captured (or modeled) S-parameter files are used in a subsequent simulation that includes frequency points not in the data, interpolation must be performed to estimate the response at those particular frequencies. To avoid interpolation errors, frequency steps on the VNA were selected to match those used for Fourier analysis of the simulated signal; no interpolation was required.

Also, steps in magnetic field strength were selected so the phase shift was in small enough steps to be used directly for beam forming. With 10° increments, the greatest variation from desired angle would be 5° ; $\cos(5^\circ)$ is 0.996, so this approximation contributed only 0.4% variation in resultant signal strength.

A sweep of the entire 2 - 20 GHz range of the filter is shown in Fig. 6.

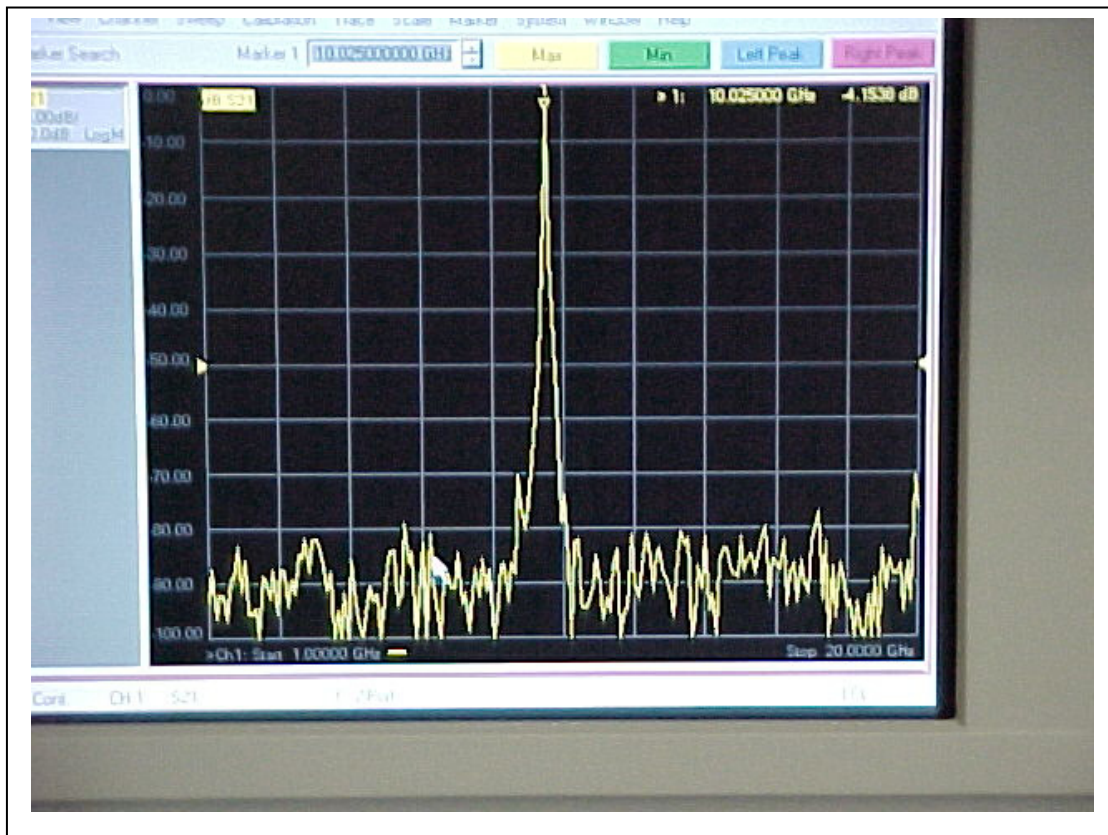


Figure 6. 2 - 20 GHz response of YIG filter

The bandpass response was measured as S-parameters over the frequency range 9.9 - 10.1 GHz and shows the YIG filter's 50 MHz bandwidth at -3 dB. Five representative

sweeps were taken to demonstrate how tuning moves the -3 dB cutoff points as it shifts the phase (see Fig. 7).

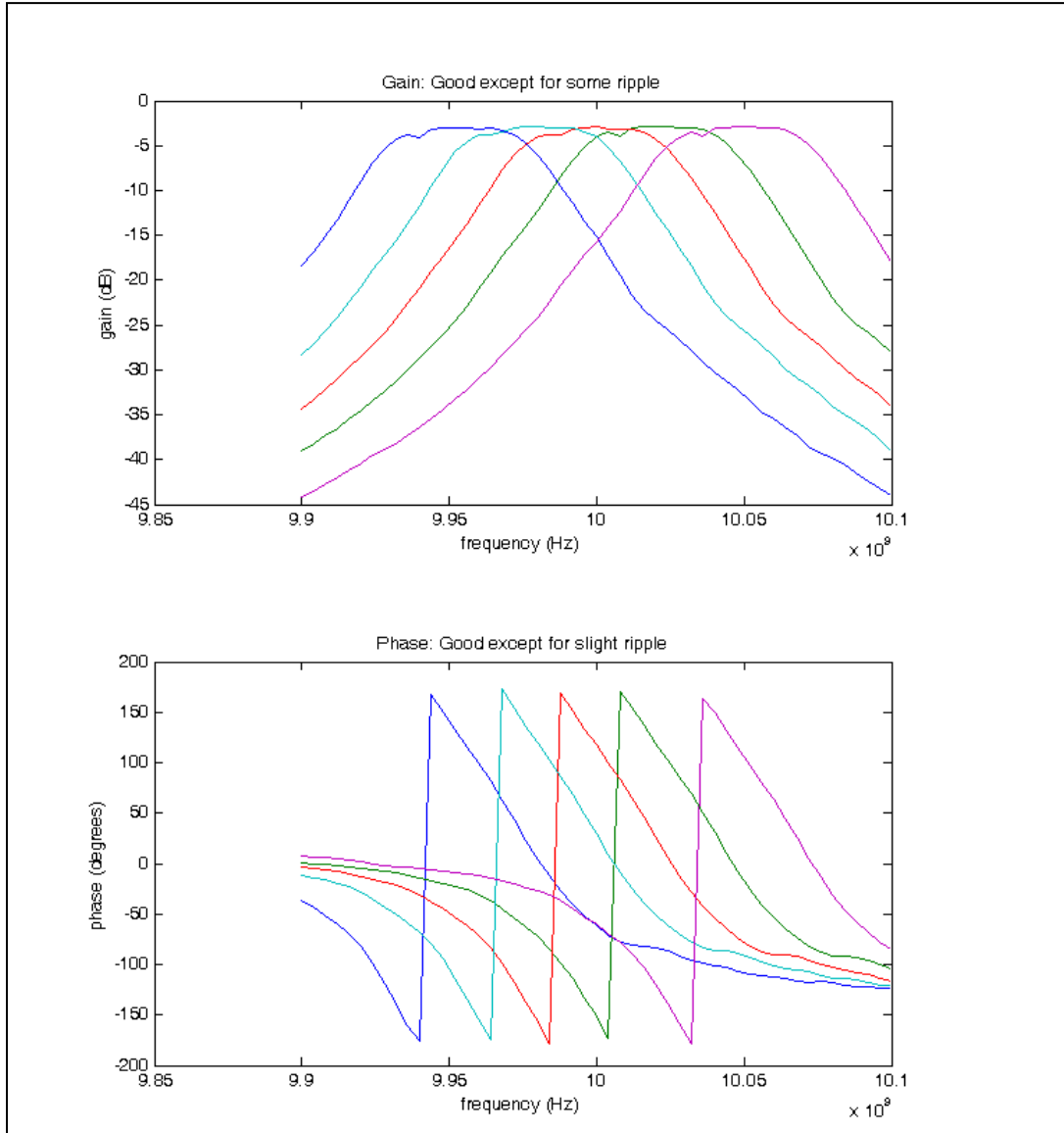


Figure 7. Measured gain and phase of YIG filter across the pass band

It is clear from this plot that shifting the center 10 GHz frequency from a -180° to $+180^\circ$ phase shift will cause greater than the desired 3 dB attenuation. The YIG filter selected is not a high enough order filter (i.e., does not have enough YIG sphere stages) to provide the desired phase shift. The radio bandwidth used in this study, 25 MHz, is relatively narrow. Still, at ± 12.5 MHz from the center frequency, the attenuation is greater. Calculations of the impact on this attenuation on radio performance were made for two situations – one with arbitrary beam angles, utilizing the larger phase shifts (resulting in undesirable attenuation), and again with a small angle where the required phase shifts can be accomplished with no more than 3 dB of attenuation. The latter calculation is representative of performance available from a YIG filter with greater bandwidth.

In the plot of gain, there is a ripple in the pass band. This was at first thought to be caused by adapters used between 2.4 mm test ports and SMA connectors on the YIG filter because their physical length was close to the wavelength in question. However, it can be seen in this plot that the ripple changes frequency as the filter is tuned. It is part of the tunable filter itself and not part of the fixed hardware.

S-parameter measurements were taken with a frequency sweep consisting of 51 uniformly spaced points from 9.98779 GHz to 10.01220 GHz, precisely matching the (lowest 25 MHz bandwidth) up-converted frequency points produced by Fast Fourier Transform (FFT) of the data stream. The filter was tuned to produce 10° increments of phase shift and data gathered at each of 36 settings (see Fig. 8).

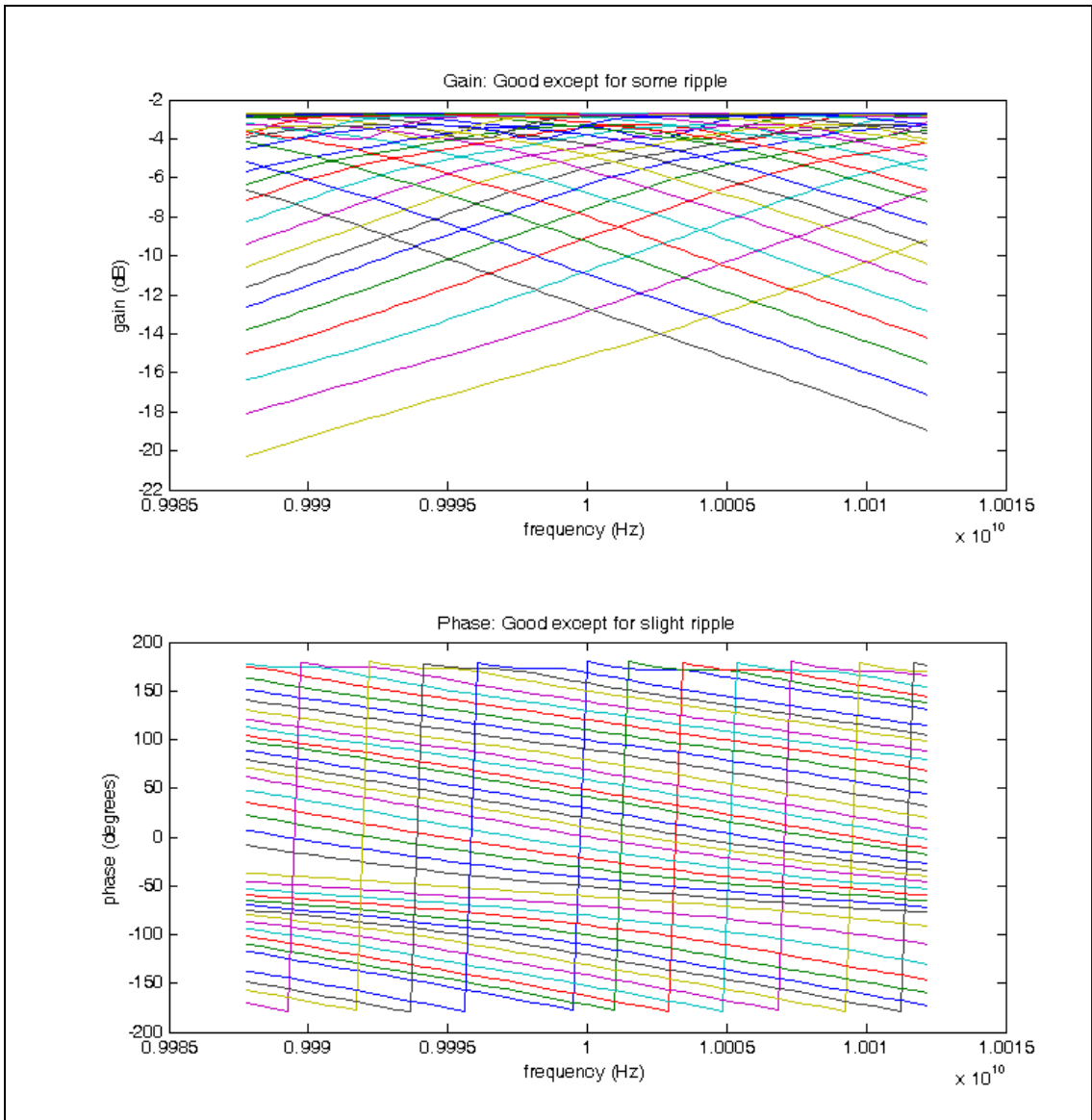


Figure 8. Measured gain and phase of YIG filter across frequency band of radio

The phase for some crossed over from -180° to $+180^\circ$, as expected. The ripple shown in phase was undesirable; this non-linearity in phase response over frequency was

one of the sources of distortion in the modulated data. Some of the gain waveforms also showed a ripple, coincident with the phase ripple.

For use as a phase shifter, it was desired to achieve a phase shift of $\pm 180^\circ$ for the nominal 10 GHz operating frequency and maintain gain flatness within 3dB across a 25 MHz bandwidth centered at nominal. For some of the tuned phase shifts, this filter produced a gain output ranging from -10 dB down to -21 dB. The significance of the reduced gain is that antenna elements fed with that signal received power -6 dB (1/4 power) or lower compared to the other elements, and therefore did not contribute appreciably to the transmitted wavefront. For a receiver application, only 1/4 or less of the power received by that element was utilized. In either transmit or receive applications, the attenuation reduced signal strength and directionality.

The available phase shifts with no more than 3 dB additional attenuation (in addition to the peak -2.6 dB response) were from $+60^\circ$ to $+180^\circ$ ($+180^\circ$ and -180° being the same). In order to show the radio performance with a YIG phase shifter that provides the desired bandwidth and phase shift, modeling was performed utilizing this limited range, which provides 120° of adjustment in phase shift, or 0.333 lambda. An antenna array with 15 elements separated by 1.0 lambda, with 120° of adjustment in phase shift, can sweep through a 1.27° angle. While this angle is small and the beam may not appear different from one generated by antenna elements that are in phase, this calculation does incorporate the frequency-dependent attenuation of the YIG filter within the pass band.

V. THE BEHAVIOR OF PHASED ARRAYS

Phased array antennas provide increased transmitted signal strength (or receive sensitivity) by introducing a phase shift between signals to or from each antenna element so the waves will have constructive interference in the desired direction due to alignment of phase as shown in Fig. 9.

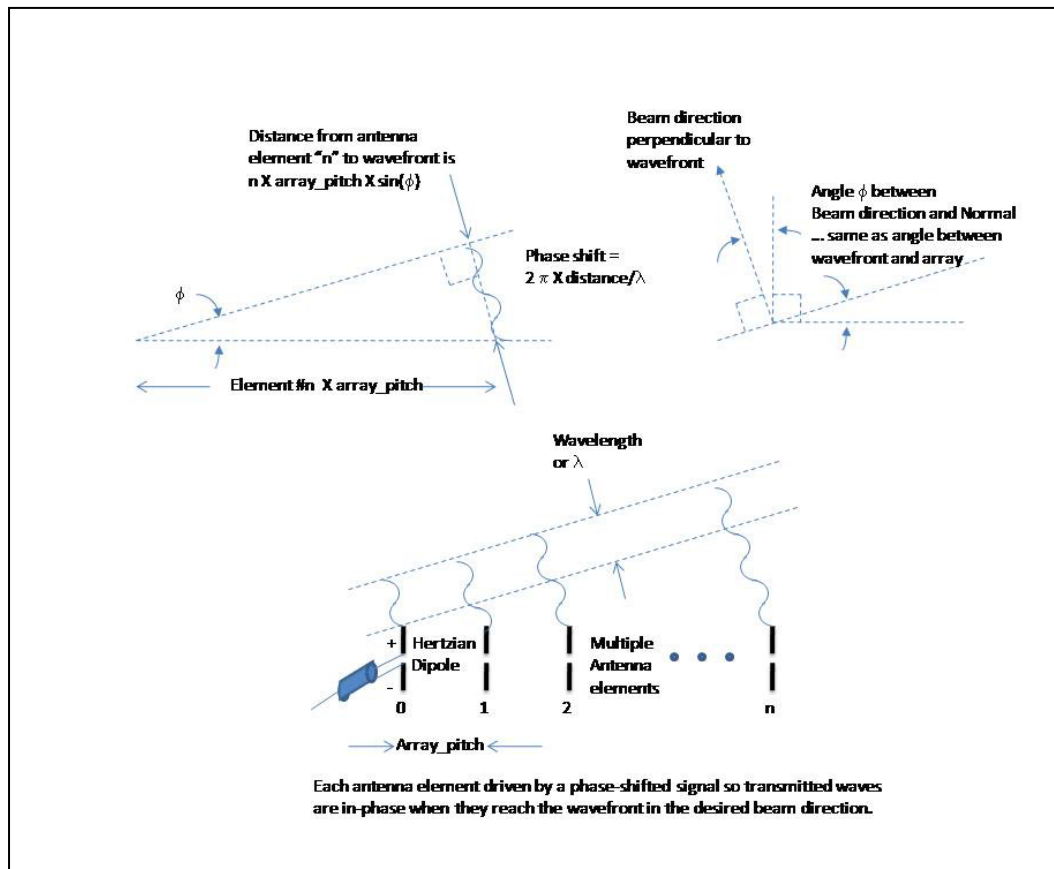


Figure 9. Phase shift vs. beam angle

This also causes reduced signal strength (or sensitivity) in other directions. However, there are many smaller lobes of increased signal strength in the radiation pattern at angles other than the desired beam direction where some of the waves again arrive in phase and cause constructive interference. Where the waves interfere destructively the signal strength is reduced. The total energy transmitted is the sum of what each antenna emits, but more of it is delivered in the beam direction. The ratio of peak energy (in the beam direction) to what would be delivered by a spherical radiator that delivered equal energy in all directions is referred to as “gain” of the antenna.

VI. SIMULATION OF RADIATION PATTERN

A notional phased array antenna system was described in Matlab. It was implemented as a one-dimensional array of elements. The constructive and destructive effects of waves propagating from each element were combined to produce a three-dimensional model. The phase-shifted signal produced by each antenna element was further shifted according to (3) and then added to the wavefront produced by the other antenna elements.

$$delayed_wave = e^{-j\omega t} \times transmitted_wave \quad (3)$$

(All dimensions were described in terms of wavelength or λ , and phase angles which are the same as ωt were used to compute changes to the waveform.) Equation (4) from Ulaby [6] describing the three-dimensional radiation pattern of a Hertzian dipole was then multiplied by this model, generating the radiation pattern for the entire phased array system.

$$F(\theta, \varphi) = \sin^2\theta \quad (4)$$

This analysis was limited to Continuous Wave (CW) signals, a pure sine wave at the carrier frequency. The radiation pattern may differ at other frequencies within the radio system bandwidth about the carrier frequency due to non-idealities of the phase shifter; this is addressed by analysis of the distortion in modulated signals, which are affected by differences in both amplitude and phase between frequency components of the signal. Using this approach, beam forming with various phase shifters was compared. In

particular, the relative gain for an ideal (perfect) phase shifter (see Fig. 10), a 3-bit delay line phase shifter (see Fig. 11), and a YIG phase shifter (see Fig. 12) were compared.

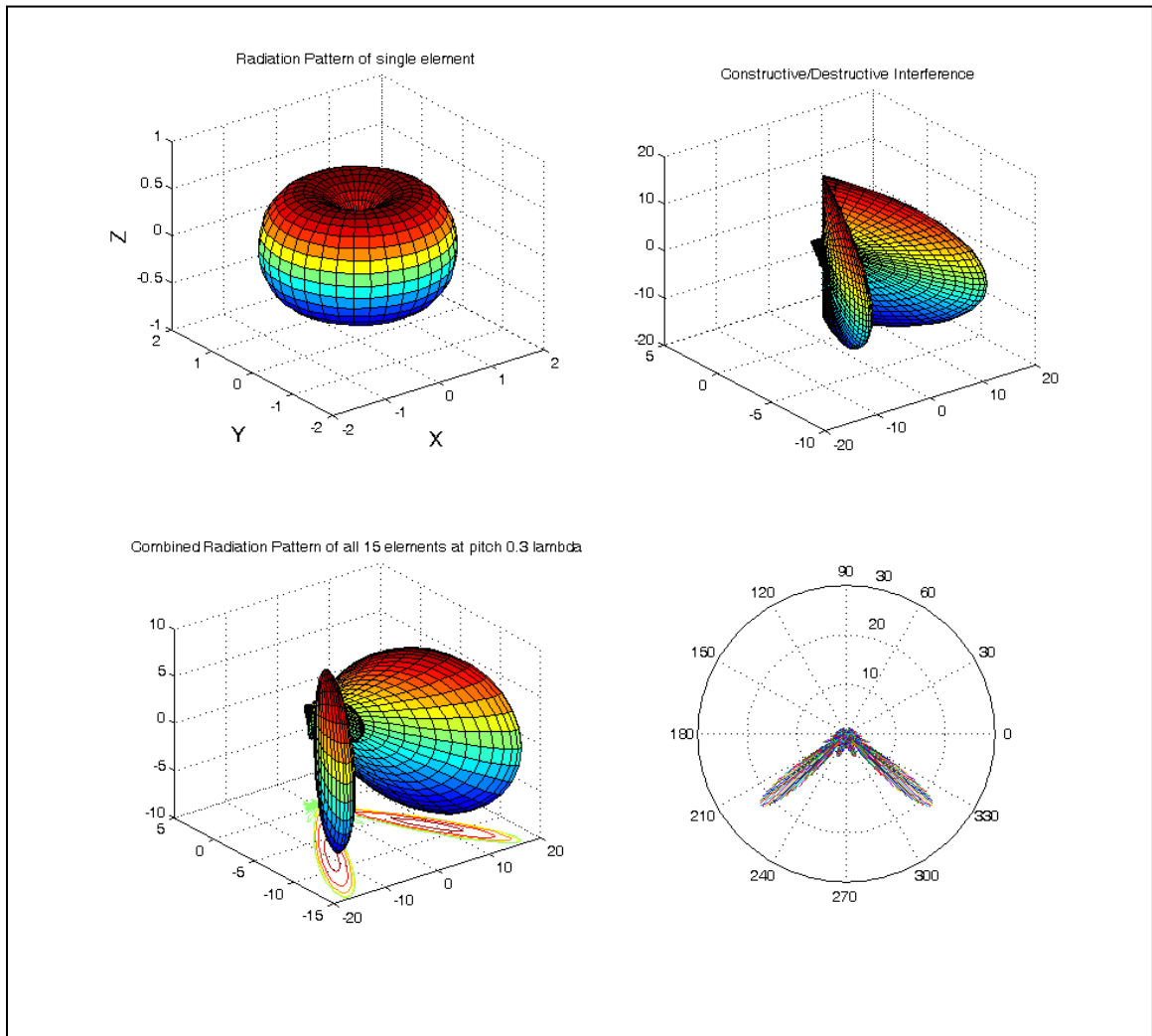


Figure 10. Radiation pattern with ideal phase shifters

Note that due to symmetry, there is a beam formed “behind” the antenna array mirroring the beam in front.

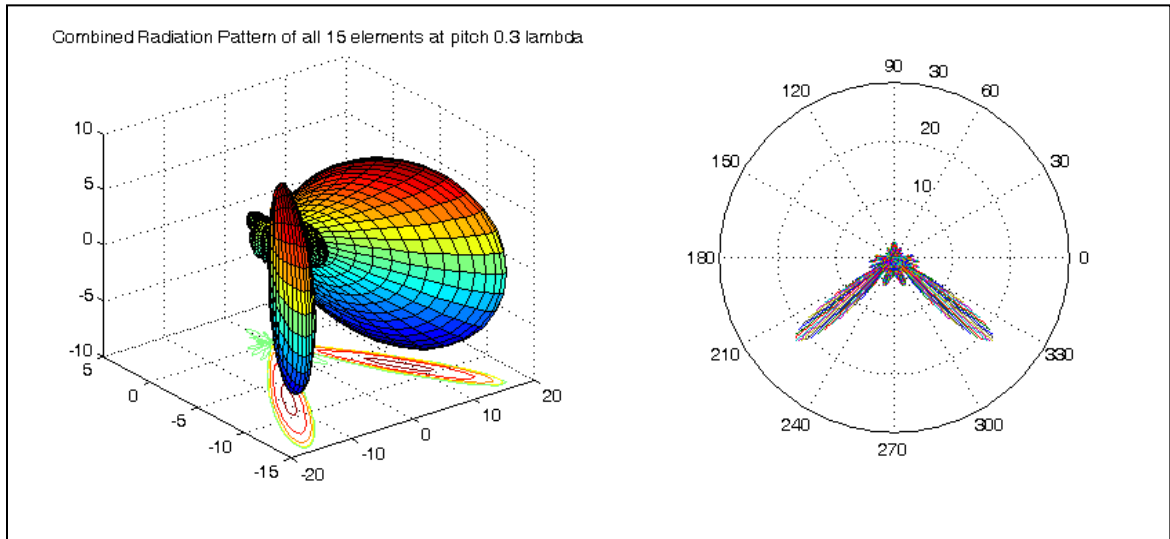


Figure 11. Radiation pattern with 3-bit phase shifters

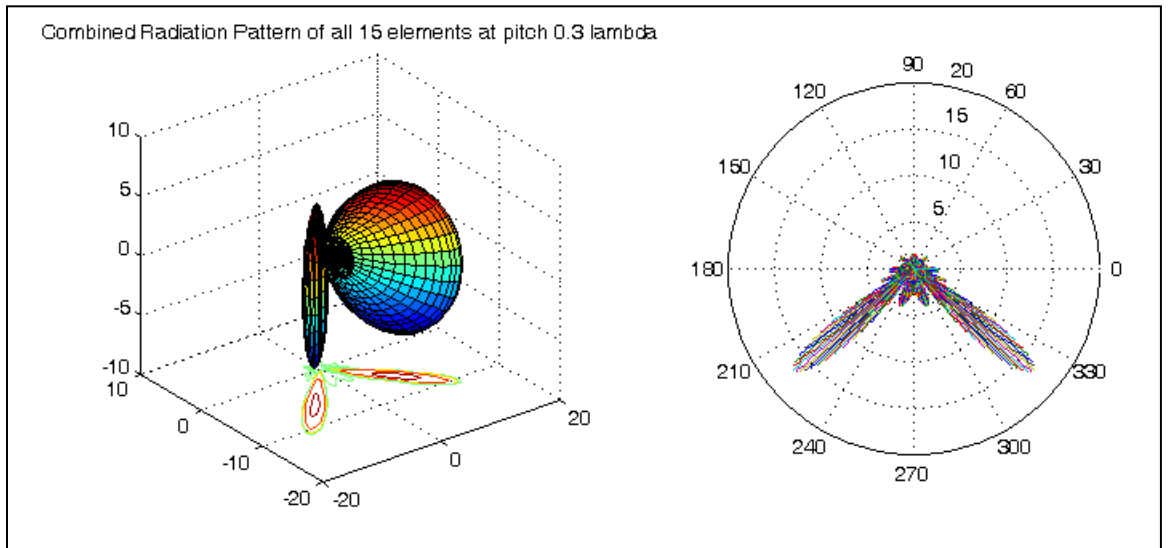


Figure 12. Radiation pattern with YIG phase shifters

With an ideal phase shifter, the beam produced at a 40° angle from an array of 15 antenna elements showed gain of 22.5, which means the field strength at the point of strongest field was 22.5 times what an omni-directional radiator would produce. This is the expectation for the perfect case; 15 elements in perfect phase multiplied by the 1.5 gain of the Hertzian dipole.

When a 3-bit (45°) phase shifter was used instead, the gain was 21.9, so the penalty for adjusting phase in these larger increments was only 3%. This shows that part of the hypothesis of this project, that precise control of phase shift would provide a more directional beam than is possible with fixed delay lines, is not correct. YIG may still offer a benefit in tuning speed, however.

With the YIG phase shifter, the gain was just 16.8. This was not due to error in phase shift, but rather due to attenuation when the phase shifter was used outside its pass band. The response of the S-parameters was normalized to 0 dB at the center of the pass band to represent an amplifier restoring the lost signal strength, but for some phase shifts the signal was attenuated by a considerable amount. If a higher order filter with sufficient bandwidth had been used, all antenna elements would have received a signal between 0 dB and -3 dB so the gain would have improved, but still below that of the lossless ideal or 3-bit delay line based phase shifter designs.

VII. SIMULATION OF MODULATION/DEMODULATION AND ERROR VECTOR MAGNITUDE

A perfectly formed phased array system with ideal delay lines feeding each element, or a dish antenna, would deliver modulated and up-converted signals without further distortion except for group delay resulting from propagation through the atmospheric medium. With any physical realization of phase shifters, however, additional group delay and frequency dependent attenuation is introduced. This issue is the primary focus of the work presented here.

G. Baseline model of digital radio with ideal channel

First, a baseline model was created in Matlab. The order of modulation and bit stream length was selected for convenience of simulation and presentation. The modulation was QAM-16, and a bit stream 16 symbols long was simulated. Higher order modulation would likely be used for high data rates in practical systems. However, techniques to reduce inter-symbol interference could be required. For this work, the lower order modulation permitted the bit stream to be recovered and EVM quantified. Then, the additional EVM resulting from a different channel (in this case imperfect phase shifters) could be determined. Likewise, the bit stream length selected was relatively short so resultant modulated waveforms could be easily presented. Longer bit streams provide all possible cases of inter-symbol interference, for instance 2^{20} bits which might be used on a Bit Error Rate (BERT) tester that operates with hardware running at full channel speed. With a large number of bits and the actual non-ideal behavior of a system, a constellation diagram for the modulated data shows blurring of spots, a graphical representation of

EVM. Using a string of just 16 symbols and the repeatability of mathematical modeling, each symbol was recovered as a single I/Q value, and these errors were combined by Root-Sum-Square (RSS) to generate an EVM. Predictably, “easy” bit streams with small changes in I and Q values produced lower EVM, and “hard” bit streams with large jumps in I and Q values produced higher EVM.

QAM-16 modulation is represented as 16 points, in a 4x4 array, and encodes 2^4 or 16 bits represented in hexadecimal as 0, 1, 2, 3, 4, 5, 6, 7, 8, 9, A, B, C, D, E, F. To modulate the data, each symbol is separated into the low two bits, which index into the X or I axis of the modulation, and the high two bits, which index into the Y or Q axis. For instance, “B” is “0111” in binary, so the low bits “11” designate the rightmost column of the 4x4 array, and the high bits “01” second row from the bottom. The I and Q values were then converted to a gain factor (to multiply with a 1.0V signal) centered at 0.0, so “00” would be represented as -1.5V, “01” as -0.5V, “10” as +0.5V, and “11” as +1.5V. (see TABLE I.)

TABLE I. I AND Q ENCODING OF SYMBOLS

		C	D	E	F
	+1.5 11	(1100)	(1101)	(1110)	(1111)
	+0.5 10	(1000)	(1001)	(1010)	(1011)
Q	-0.5 01	(0100)	(0101)	(0110)	(0111)
	-1.5 00	(0000)	(0001)	(0010)	(0011)
		00	01	10	11
		-1.5	-0.5	+0.5	+1.5
			I		

A time-domain representation of 12.5 MHz 1.0V sine and cosine signals was created, with 20 data points per cycle as the un-modulated baseband signal. The I and Q representations of each bit were used to scale a single cycle of the signal, which were then added together and concatenated with the waveform representing the next cycle. The data rate was therefore 4 bits x 12.5 MHz or 50 Mbps. Because it was recognized that the sine wave used for I modulation would switch between symbols when crossing zero volts, while the cosine wave for Q modulation would switch at maximum value, both were offset by 45° to balance the amount of high-frequency energy generated in each. Rather than

one having a value of 0.0V and the other having a value of 1.0V at the point in the waveform where amplitude is changed, each has a value of 0.707V. (An even better approach might have been to delay the Q part of the symbol by 45° so both switch at 0.0V. While that would eliminate voltage discontinuities in the modulated signal, the derivatives would still be undefined, so energy in frequencies outside the channel bandwidth could not be completely eliminated.) An FFT (Fast Fourier Transform) was then performed to generate a frequency-domain representation of the time-domain modulated signal.

The modulated signal was treated as having been up-converted to the target 10 GHz X-band frequency. A physical mixer used for this purpose would necessarily introduce distortions in-band from third-order harmonics, but as a model of an ideal mixer, the time axis of the FFT data was simply changed.

To check behavior of the model, the data was converted back to baseband, assuming the channel had unlimited bandwidth. That is to say, all frequency components in the FFT data were used to recover the time-domain modulated data, and it was subsequently demodulated. The I and Q components reproduced the input bit stream and had errors on the order of 10^{-15} , representing only mathematical rounding errors. The frequency data was then truncated beyond 25 MHz bandwidth with an idealized brick wall filter. The data was still recoverable, but this time EVM ranging from 6.8% to 35.9% resulted depending on the bit stream. This was used as a baseline for comparison with non-ideal channels representing phase shifters and the summing of wave-fronts from them.

While it is readily apparent that the distortion produced by the bandwidth-limited idealized channel would be too high to support reliable communication at higher symbol rates or with higher order modulation like QAM-64 or above, because the same magnitude error would represent a higher portion of the inter-symbol spacing, normal design techniques would reduce the distortion. In particular, the abrupt transitions in I and Q values could be digitally filtered to reduce high frequency content, and the final level could be adjusted to compensate depending on the previous symbol. This could be performed either before transmission or after reception. Only the additional error introduced by the phase shifter should be considered representative of an actual system, and not that of the modeled communication system used as a baseline.

One bit stream what was tested was [56A9401237BFEDC8], which was selected because the magnitude of transitions is minimized, and the order of bits as displayed in the modulation constellation is easy to follow (see Fig. 13). It has minimum high-frequency content, and is useful as an example because the bit sequence can be matched to graphical representations of the I and Q bit stream.

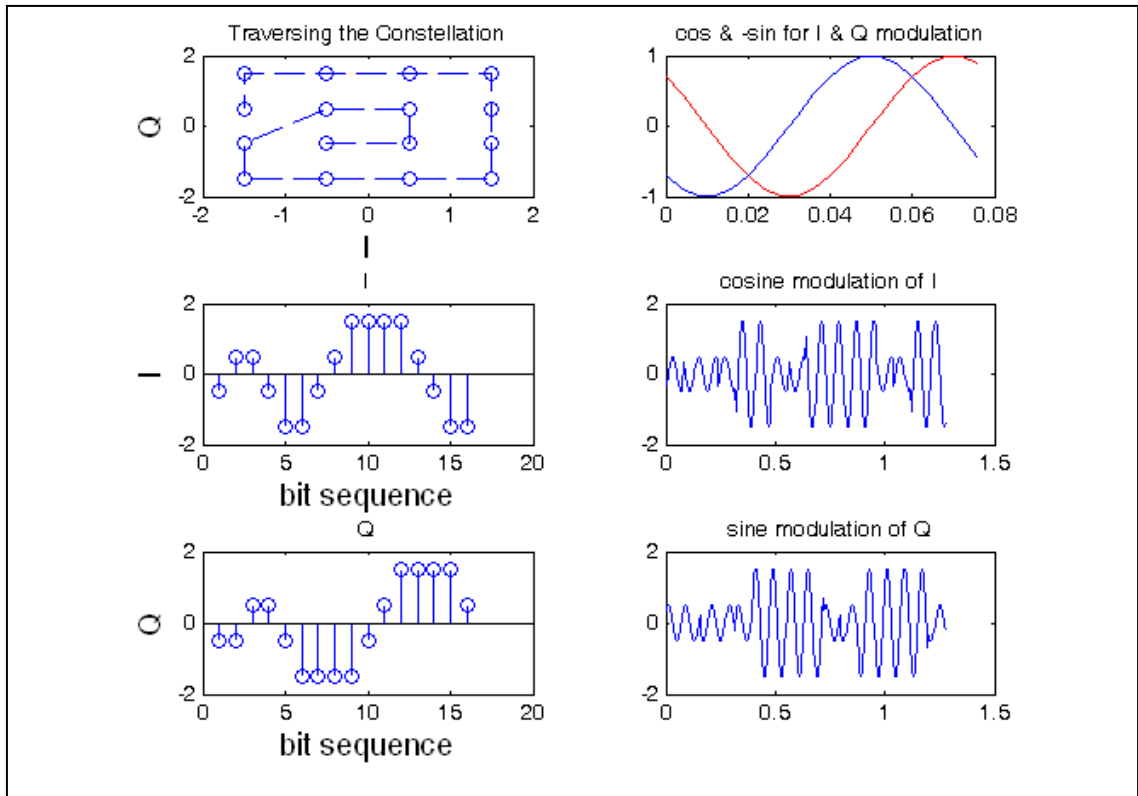


Figure 13. Constellation and I/Q modulation of [56A9401237BFEDC8]

The resultant QAM-16 modulation, RF frequency content of baseband, and a 25 MHz low pass filter (applied to the baseband, but equally representative of a band-pass filter from 9.9875 GHz to 10.0125 GHz applied after mixing with LO to shift the signal up to X-band) are shown in Fig. 14.

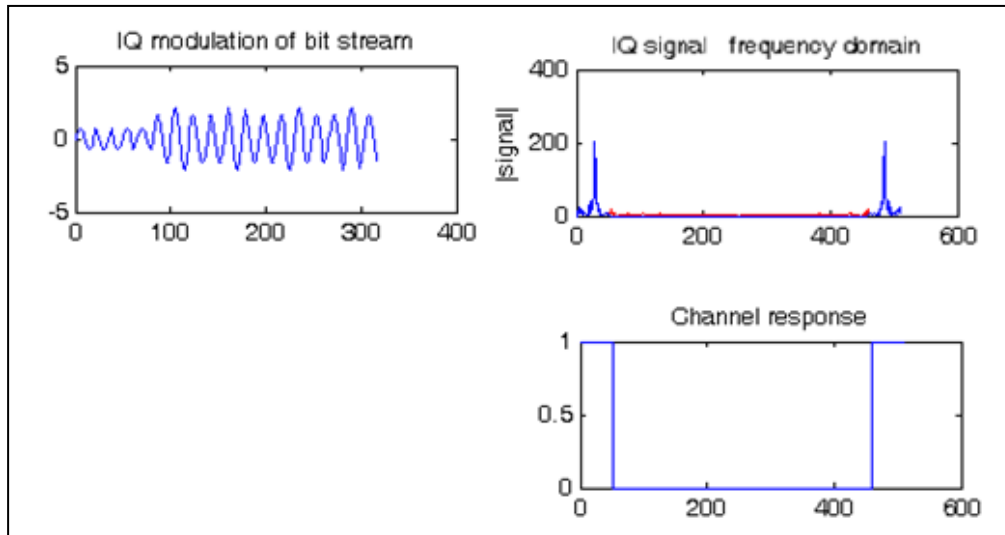


Figure 14. QAM-16 modulation and frequency content of [56A9401237BFEDC8]

The abscissa of each graph is points in the data array – 320 samples for the time-domain waveform, and 512 frequency points from an FFT computed on it. Note that data generated by Matlab includes both positive and negative frequencies, but instead of placing negative frequencies to the left of zero (which represents DC), the negative frequencies are presented to the right of the highest positive frequency. The 26th point in the frequency array, above which the brick wall filter cut off output, was at 24.9 MHz in the baseband. For the link bandwidth to be made wider it would be necessary to increase the baseband frequency. Because 12.5 MHz was selected, with a local oscillator (LO) frequency of 9.9875 GHz, the modulated data is centered at 10.0 GHz (5), but also replicated at 9.9750 GHz (6); if bandwidth greater than +/- 12.5 MHz from baseband was permitted into the mixer these two would overlap.

$$f_{LO} + f_{BaseBand} \quad (5)$$

$$f_{LO} - f_{BaseBand} \quad (6)$$

Recovery of modulated data requires synchronization with the timing of symbols in the signal. For amplitude modulation, it also requires proper adjustment of gain. Actual implementation of a system would use a phase-locked loop (PLL) to synchronize the signals used for down-converting and demodulation. For this analysis delay was manually added so demodulation is synchronized with transitions in the bit stream. Otherwise, each symbol would be incorrectly recovered as a combination of levels taken from two adjacent symbols. Similarly, phase shift associated with the delay would interfere with recovery of I and Q within the symbol.

The received baseband signal was separated into time slices the length of a single symbol. Each was then multiplied by sine and cosine waves and the mean computed, recovering the levels of the respective I and Q signals (see Fig. 15).

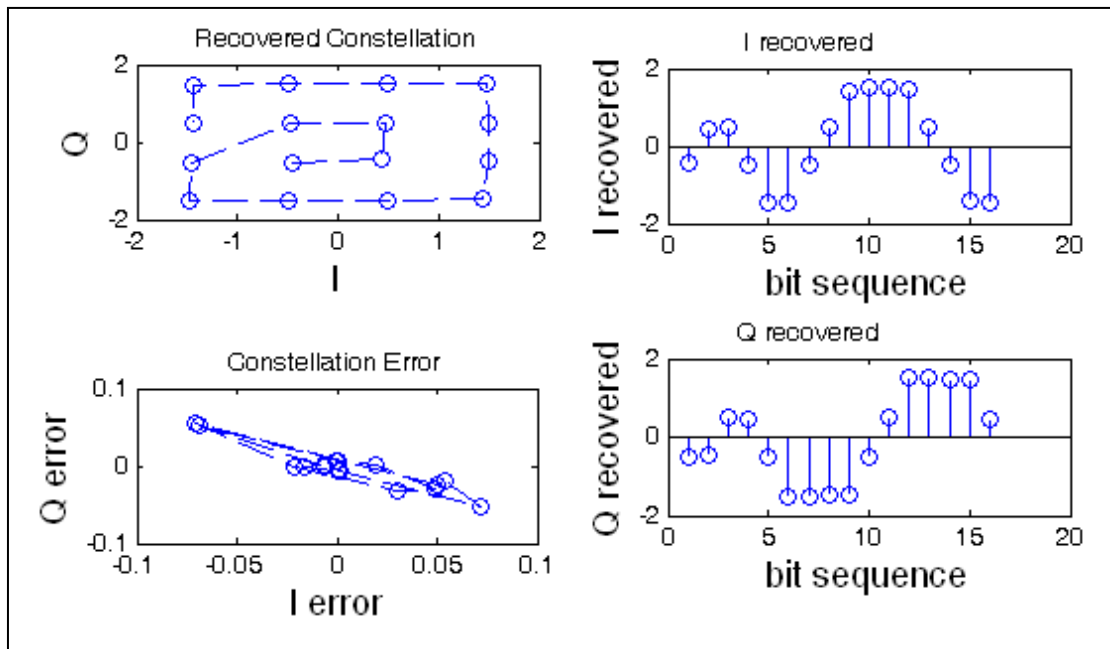


Figure 15. Recovered constellation, I & Q, and error for [56A9401237BFEDC8]

The error, or deviation from transmitted levels, was determined and combined by the RSS method to produce an EVM, 6.8% in the case of this bit pattern which spiraled through the 16 symbols. It can be clearly seen that the recovered I, Q, and constellation are slightly distorted but are easily recognizable as representing the original data.

The same test was re-run with a symbol sequence chosen to maximize high frequency content, alternating back and forth between opposite sides of the constellation [0F4B87C3D2E1A569] (see Fig. 16).

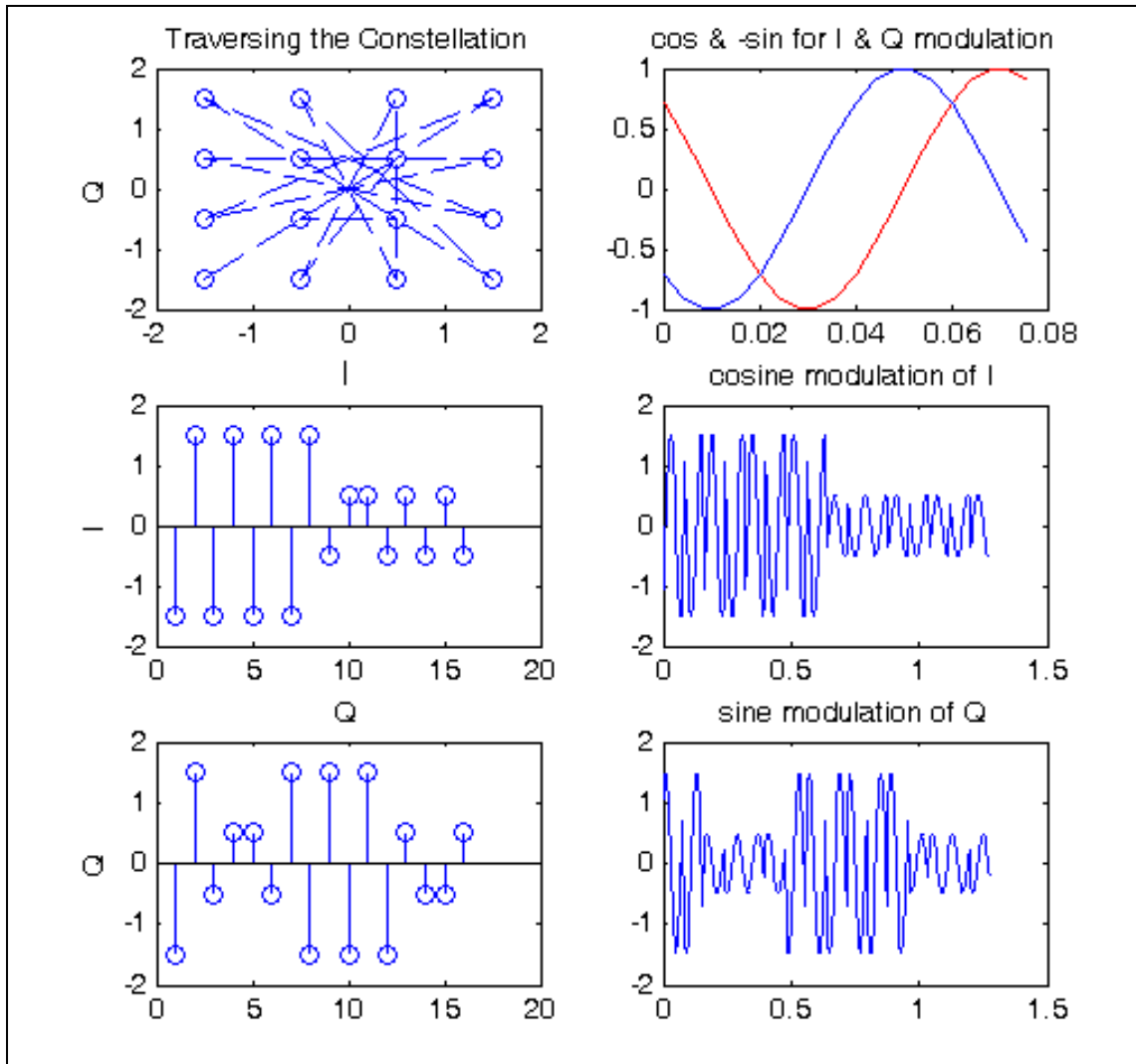


Figure 16. Constellation and I/Q modulation of [0F4B87C3D2E1A569]

The resultant QAM-16 modulation and frequency content are shown in Fig. 17.

Significantly more high frequency content is seen as expected. The frequency content lost due to 25 MHz channel bandwidth is presented in red, while the preserved content is presented in blue.

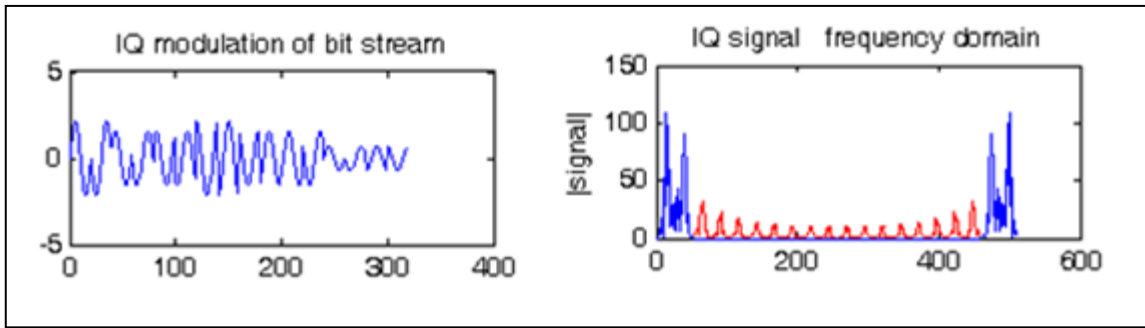


Figure 17. QAM-16 modulation and frequency content of [0F4B87C3D2E1A569]

The recovered constellation and I & Q data shown in Fig. 18 have significantly more distortion as is to be expected due to the greater amount of high-frequency information which is outside the bandwidth-limited channel.

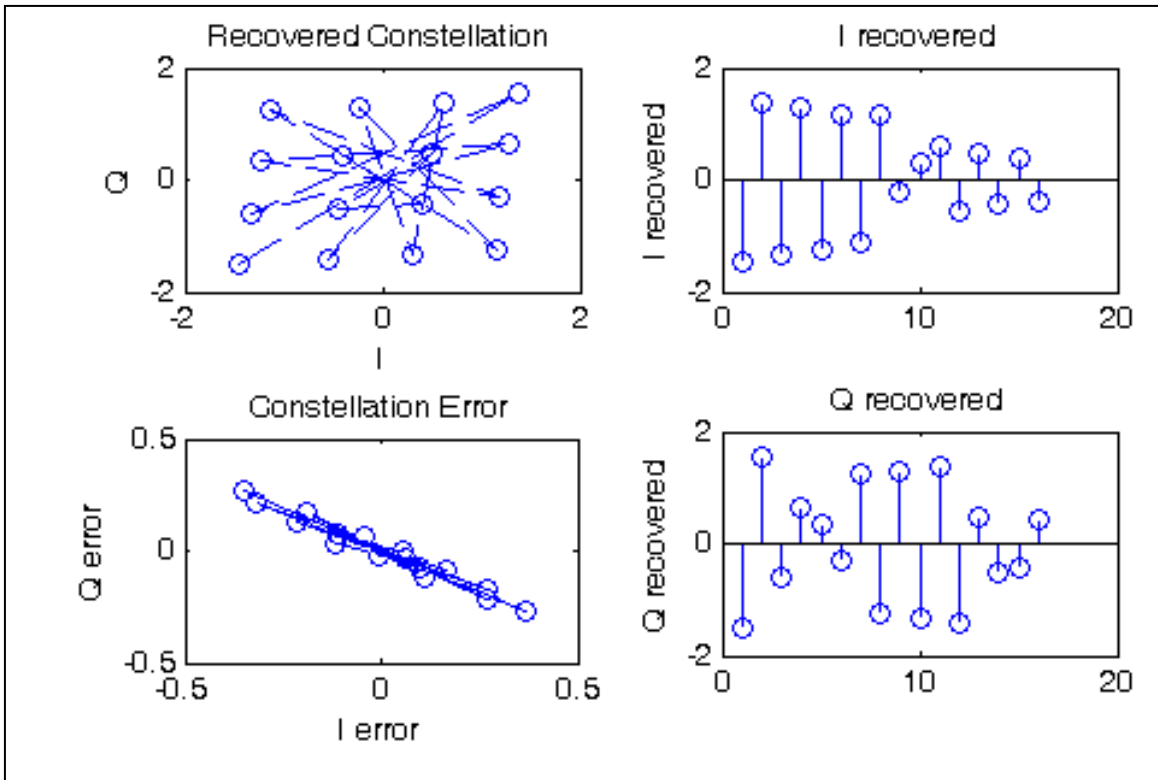


Figure 18. Recovered constellation, I & Q, and error for [0F4B87C3D2E1A569]

This time the EVM is 35.9% (providing 37.5 MHz bandwidth would reduce it to 19.3%). Because the maximum error in the constellation is less than 0.5 (half the separation between symbols) in both I and Q, 100% of the data is recovered correctly.

H. Three-bit phase shifter for beam forming

The simulation was repeated for the symbol sequence [0F4B87C3D2E1A569], this time utilizing the 3-bit (45° increment) phase shifter (See Fig. 19) .

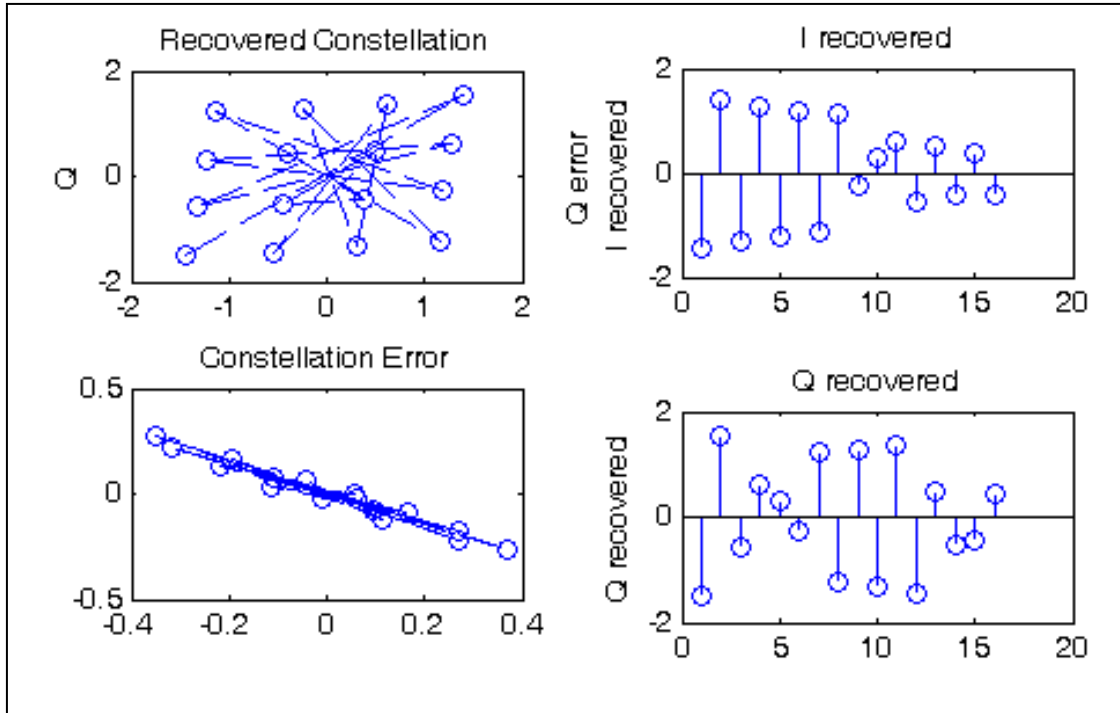


Figure 19. Recovered constellation, I & Q, and error, 3-bit phase shifter

The EVM was again 35.9%. Note that the delay line model used was lossless and introduced no distortion due to group delay; it represented ideal switches and transmission lines.

1. Ideal Butterworth filter phase shifter for beam forming

Prior to measuring an actual phase shifter, a Matlab model of an idealized phase shifter was developed based on the Butterworth approximation. Eighth-order high-pass and low-pass filters were combined. The transfer functions for cutoff frequency of 1 radian/second were given by (7) for lowpass and (8) for highpass.

$$\frac{1}{(s^2 + 0.3902s + 1)(s^2 + 1.1111s + 1)(s^2 + 1.6629s + 1)(s^2 + 1.9616s + 1)} \quad (7)$$

$$\frac{s^{-8}}{(s^{-2} + 0.3902s^{-1} + 1)(s^{-2} + 1.1111s^{-1} + 1)(s^{-2} + 1.6629s^{-1} + 1)(s^{-2} + 1.9616s^{-1} + 1)} \quad (8)$$

For zero phase shift, the highpass was set to provide a low frequency cutoff of 6.67 GHz, and the lowpass was set to provide a high-frequency cutoff of 15 GHz. By adjusting the center frequency above or below nominal, phase shift from -180° to $+180^\circ$ could be achieved as shown in Fig. 20.

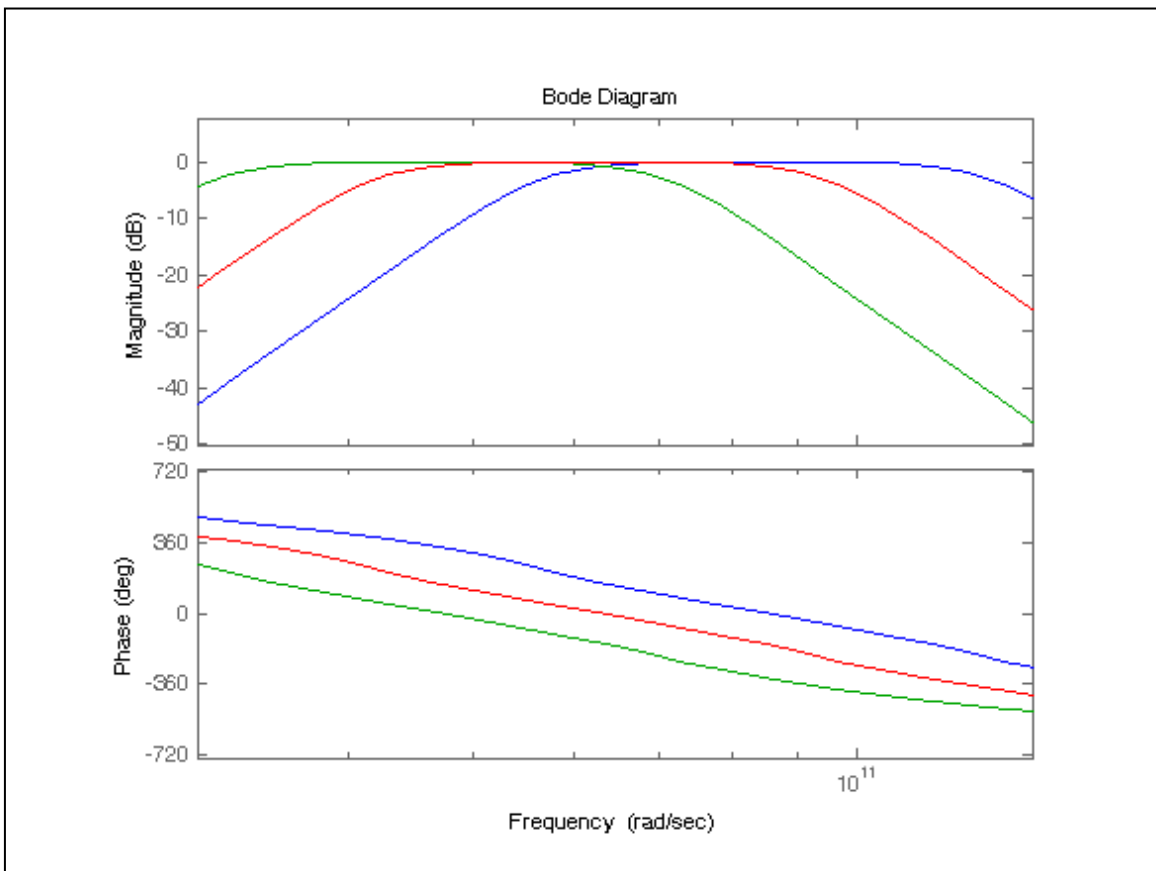


Figure 20. Butterworth bandpass filter tuned around 10 GHz to provide phase shift

Wave-fronts from multiple phase shifters were combined according to the phase at which they would arrive from a remote antenna in the direction of beam orientation. A one-dimensional array of 15 antenna elements separated by one lambda (wavelength) at the nominal 10.0 GHz frequency was modeled. A simulation was performed with phase shifts forming a beam with 40° orientation. In an actual radio, Automatic Gain Control (AGC) would maintain the received signal at levels suitable for analog processing, and gain as well as phase would be adjusted for optimum recovery of modulated symbols. As a simplification in this model, the channel response was normalized to a gain of 1.0 at nominal frequency, and delay (implemented as additional phase shift) was added to provide synchronization with the demodulator. The recovered constellation and I and Q modulation are shown in Fig. 21.

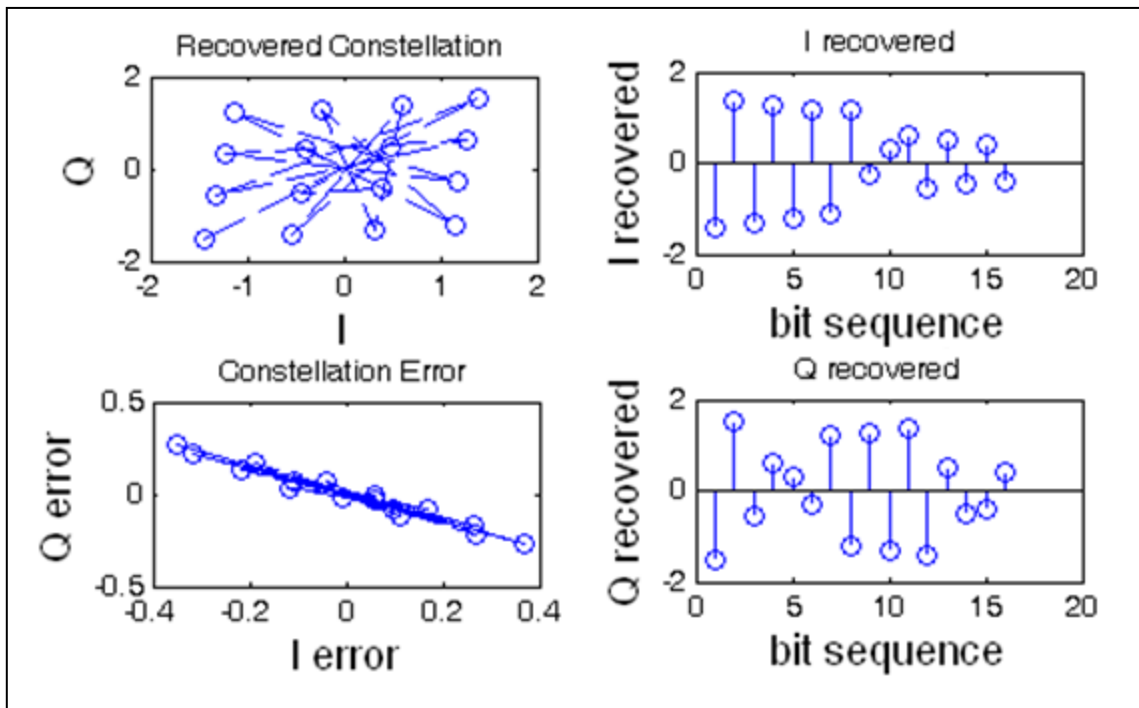


Figure 21. Recovered constellation, I & Q, and error, Butterworth phase shifter

This time the EVM was 35.7%. This is actually slightly less than with the baseline channel. It probably represents very little additional distortion, and that which did occur happened to improve one of the heavily counted outlying points in the constellation error. The code was then modified to compare with a constellation baseline recovered from an ideal (but 25 MHz bandwidth limited) channel rather than the transmitted constellation. When compared to the baseline recovered constellation the EVM contribution from the ideal Butterworth phase shifter was found to be 0.22%.

J. Measured YIG filter phase shifter for beam forming

The simulation of beam forming was repeated, this time using measured S-parameter files from the YIG filter as phase shifters. Unlike the ideal filter, the YIG filter had 2.6 dB of attenuation when the center of the pass-band was tuned to the nominal 10.0 GHz operating frequency. When tuned off-nominal to effect a phase shift, the loss was greater, as much as -20 dB. These variations decrease directionality as shown in the radiation pattern, but for analysis of the digital radio, there are two considerations: the attenuation reduces gain (or signal strength), and frequency dependent attenuation distorts the modulated data. Overall attenuation did not figure into the results calculated because gain was normalized back to 1.0 at nominal frequency to implement automatic gain control required to demodulate and recover the data. In an actual system, reduced RF signal strength would increase EVM due to decreased signal to noise ratio (SNR). Frequency dependent gain, as well as variations in frequency dependent phase shift, distort the modulated signal and contributed to EVM in the recovered constellation, and that distortion is the focus of this work. In the recovered constellation skewed positions of I and Q reflect the total distortion which primarily came from the 25 MHz bandwidth-limited channel. The delta in constellation error shown was generated by comparing the recovered constellation with what was recovered from an ideal but bandwidth limited channel, and represents the impact of the YIG phase shifter (see Fig. 22).

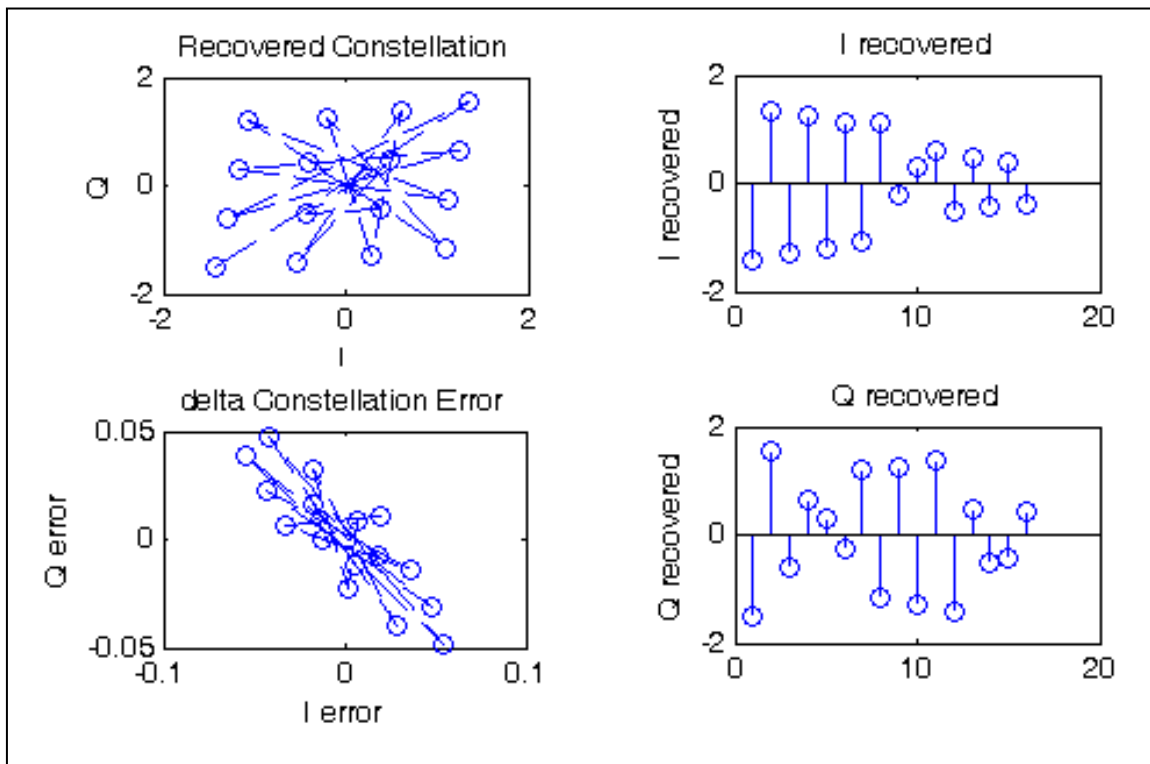


Figure 22. Recovered constellation and delta error YIG vs. baseline

This time the EVM was 41.6%. The recovered I and Q signals were compared to what was recovered from an ideal but bandwidth limited channel, and the EVM contribution from the YIG phase shifter was found to be 6.0%. Originally it had been expected that the EVM contribution from the bandwidth-limited channel and from the YIG phase shifter would combine by the RSS method, which is appropriate when multiple sources of error are independent. When combining 0.359 with 0.060 by this method as shown in (9), the result is 0.364, or 36.4%.

$$\sqrt{0.359^2 + 0.06^2} = 0.364 \quad (9)$$

A linear combination of 35.9% and 6.0% indicates 41.9% EVM, almost what was produced by the model, as computed with (10), so the error contributions of the bandwidth-limited channel and the YIG bandpass filter are highly dependent on the same factor, namely frequency content.

$$0.359 + 0.060 = 0.419 \quad (10)$$

While the (ideal) bandwidth limited channel only affected frequencies outside its 25 MHz bandwidth and the YIG bandpass filter only affected the frequencies it was presented, namely those within the 25 MHz bandwidth, the amount of information present in these two frequency ranges are apparently strongly correlated.

K. YIG filter phase shifter operated within -3 dB bandwidth

The previous simulation of beam forming required phase shifts across the entire +/- 180° range, and some of the S-parameters had as much as 12.4 dB difference in attenuation across the 25 MHz frequency band, which contributed to increased EVM. To show what the performance would be with a YIG bandpass filter having more stages and a wider pass-band, a simulation was run with 1.27° beam angle which could be formed with the S-parameters representing +60° to +180° phase shift. The Matlab code originally started with +0° for the first element, but the S-parameters providing this phase shift were one of the ones with excessive attenuation, so the code was modified to start at +60°.

When re-run the EVM decreased to 4.4%. The reason the impact of the YIG phase shifter on distortion was not greater when operated beyond the -3 dB point was that the contribution was reduced; this is what caused the decreased gain when the radiation pattern was calculated. Using a YIG filter with sufficient bandwidth would do more to improve gain than EVM, as variations in gain across frequency were averaged out. It is also interesting to note that the delta constellation error appears uniformly distributed between I and Q independently (Fig. 23); there is not a correlation between I and Q error as occurred with the earlier, more highly distorting channels.

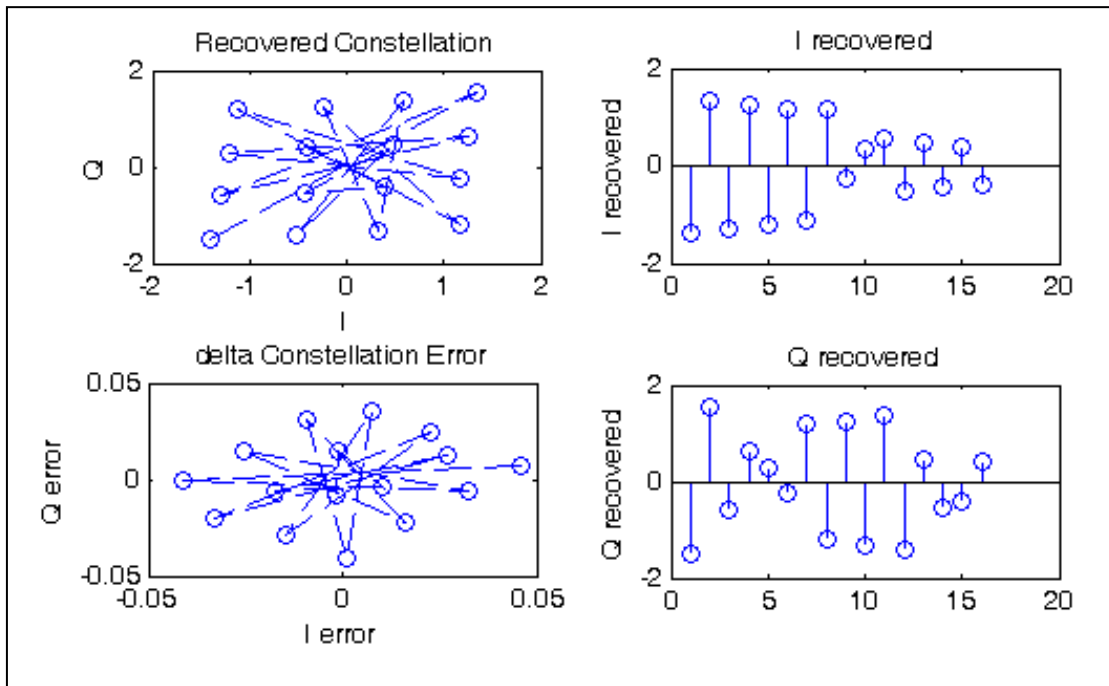


Figure 23. Recovered constellation and delta error YIG vs. baseline for small angle

L. Swept beam angle using YIG filter phase shifter

The particular amount of phase shift required at each antenna element varies with the beam angle. In the case of a 30° beam angle and antenna elements separated by one wavelength, only two phase shifts are used by all the antenna elements, e.g. just 0° or $+180^\circ$. Because attenuation (and slope of attenuation vs. frequency) from the YIG filter that was characterized was considerably greater than desired for some selected phase shifts, both signal strength and EVM vary with beam angle. A simulation was run sweeping beam angle from 0° to $+90^\circ$. The results are plotted in Fig. 24.

The EVM for 0° was higher at 12% due to the characteristics of the single S-parameter which was used for all antenna elements. Most other beam angles averaged out the non-ideal behavior of a number of S-parameters. When the code was modified so the 0° beam angle used only the center of the YIG bandpass filter, which had a $+120^\circ$ phase shift, EVM for that beam angle was reduced to 2.7%. (A lumped-element bandpass filter with zero dimensions, such as the ideal Butterworth filter described previously, exhibits no phase shift at the center of the pass band. A physical implementation such as the YIG bandpass filter has length through which the signal must propagate, introducing frequency-dependent phase shift.)

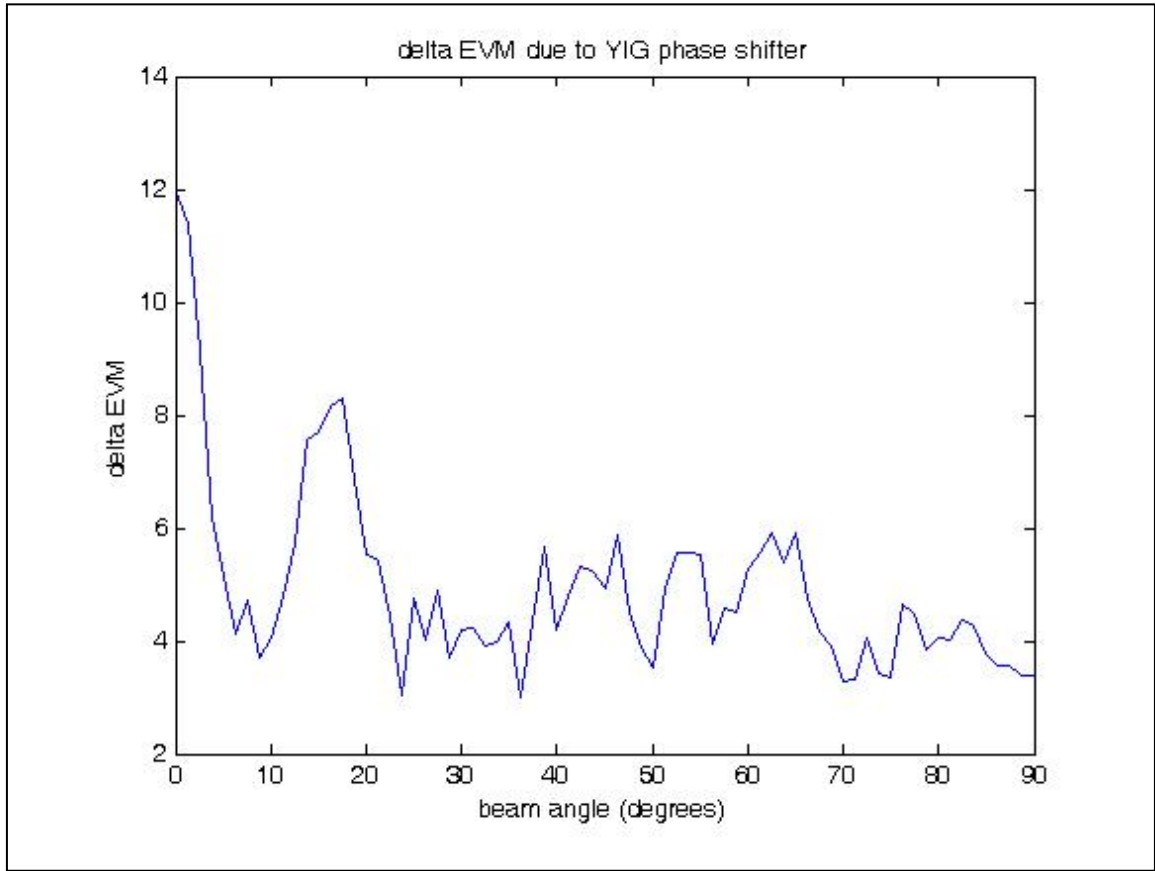


Figure 24. EVM variation as beam swept from 0° to +90° by YIG phase shifter

VIII. ISSUES IDENTIFIED IN PHASED ARRAY SYSTEMS

Phased array antenna systems are used as an alternative to dish antennas when it is preferred to have no moving parts, often for reasons of cost, maintenance, or speed of sweeping/hopping. There are important differences, however.

Even for a continuous tone, it is readily apparent that the radiation pattern has a number of side lobes where signals from the antenna elements constructively interfere. For transmitter applications this is simply lost power, but for receivers, if selectivity between transmitting sources is to be based on spatial separation rather than frequency, signals from other sources that happen to be located in the side lobes will also be received.

Modulated data is replicated over some number of cycles of the carrier frequency. For instance, in the analysis provided here, each symbol was encoded as a single cycle at 12.5 MHz (modulated and filtered such that it occupied 25 MHz bandwidth), then mixed up to 10 GHz. Accordingly, the symbol is transmitted as modulation on 800 cycles of the carrier. While all energy directed by a dish antenna would arrive at (or from) a remote antenna at the same time due to equal path length (except for group delay caused by differences in propagation velocity through the intervening medium, the atmosphere), this is not the case with phased array. Up to one cycle of phase shift might be accomplished with signal delayed by the appropriate amount, but if for instance 540° is required for an antenna element located 1.5 wavelengths further from the target than another, only 180° is provided. This provides proper constructive interference of the carrier signal, but overlaps one cycle of carrier signal carrying a given modulated symbol with a cycle of carrier

signal carrying the previous symbol. For the notional system using 800 cycles of carrier to represent each symbol, this would only be one cycle of interference vs. 799 without such corruption. However, for systems where the symbol rate is closer to carrier frequency, or where the antenna array spans a greater number of wavelengths, the effect would be greater. While the impact on EVM could be reduced by pre- or post-compensation correcting the modulation level depending on adjacent bits, such an approach would not reduce the impact on antenna gain. What would be required to fully address the issue is phase shift spanning multiple 360° cycles. This could be accomplished in the RF domain with additional stages of filter for YIG or Varactor based phase shifters or additional lengths of coax/microstrip for delay-line phase shifters. Alternatively it could be addressed in the digital domain for systems generating/recovering data from the modulated signal on a per-element basis.

Because a frequency-domain mathematical approach was taken to combine wavefronts from antenna elements, the work presented here does not incorporate the effects of overlapping modulated symbols described above. For analysis of a system where the symbol rate is sufficiently close to carrier frequency for this effect to be significant, the modulated bit stream could be shifted by a multiple of the carrier period prior to converting it to the frequency domain.

IX. POTENTIAL PITFALLS OF CHARACTERIZATION AND ANALYSIS APPROACH

The approach of measuring individual components and simulating overall system performance is convenient, but leaves open the possibility for various mistakes. A common error in SPICE simulation is to capture an output waveform from one circuit (driving an anticipated load, or no load at all), then to apply that waveform as a voltage source with zero impedance to the next stage. If the actual impedance of the next stage input is different, the applied stimulus will be incorrect. The approach taken in RF and microwave modeling, interconnecting various S-parameter blocks (or other representations) is meant to avoid such problems by presenting appropriate complex impedances. Another concern for characterization of the phase shifter is that measurements by the Vector Network Analyzer (VNA) may represent an average of multiple cycles. Averaging is useful to remove random errors or noise. However, instantaneous phase shift for a single cycle is required, because in phased array applications instantaneous waveforms from each antenna element combine to generate the wavefront.

Besides implementing an actual phased array antenna system and performing an over the air measurement, an alternative test would be to combine phase-shifted and non-phase-shifted signals. This can be performed with a splitter, followed by the phase-shifter for one channel and an attenuator for the other, and then a combiner. The attenuator models a (fixed) phase shifter by simply providing a similar loss. The measured

combination of the two channels will match the calculated combination only if the random variations in phase shift are not too significant.

X. ON IMPLEMENTING AN ACTUAL SYSTEM

For purposes of characterizing the EVM contribution of a YIG phase shifter, a notional digital radio system was implemented in Matlab, modeling idealized components. Several changes would ease implementation with actual hardware. Selecting a higher frequency IF would reduce the errors introduced by variations in LO. Prior to recovering the I and Q bitstream, the IF data sample could be analyzed to determine the precise IF frequency it contained; this would correct for oscillator variation as well as Doppler shift. Filtering and compensation would be performed to limit the channel bandwidth required and reduce inter-symbol interference.

XI. CONCLUSION

The original hypothesis, that a YIG band-pass filter providing precise phase shift would result in a higher gain phased array antenna system than one using discrete delay lines, was found not to be true. With 45° increments in phase shift there is little reduction in gain compared to ideal phase shifters.

The commercially available YIG filter selected for this work did not have sufficient phase shift in the passband to carry a 25 MHz bandwidth signal while tuning for $\pm 180^\circ$ phase shift. It was likely built with two YIG spheres rather than four; this would be consistent with the insertion loss it displayed. Despite the frequency-dependent attenuation it exhibited under some operating conditions, the simulated contribution to system EVM of around 6% that resulted suggests it would work in an actual system.

While the YIG phase shifter did not show improved beam forming compared to discrete delay line shifters, it may still be useful for rapid beam sweeping. When a large number of antenna elements is used for high gain, the beam angle will have to be changed more frequently to track a rapidly moving target. If relays are used to switch delay lines, the millisecond switching delay could result in reduced gain or having the beam off the target. A continuously variable phase shifter such as YIG (or varactor for lower frequencies) could still provide a benefit in that case.

MATLAB CODE

This section contains listings of all Matlab code used for processing and analysis of the data. It was executed under Matlab version 7.7.0.471 (R2008b).

A. Radiation pattern

The function 'plot_antenna_pattern_n_dipole' is the top level routine used to generate a surface representing the radiation pattern of a phased array.

```
function XX = plot_antenna_pattern_n_dipole
% EE299 Thesis - Test antenna_pattern routine
% Consider "n" dipoles, separated by pitch
% [x,y,z] = sph2cart(THETA,PHI,R)
% note 'PHI' is angle from X-Y plane
% i.e. straight up = 90 degrees, not 0 degrees as in Electromagnetics
% use [Matlab] PHI = 90 - [Electromagnetics] FI

disp('Antenna Elements')
```

```

pitch = 0.333 % lambda
quantity = 15 % elements in antenna array
%quantity = 4 % elements in antenna array
antenna_type = 'hertzian_dipole'
shifter_type = 'YIG'
%shifter_type = 'ideal'
%shifter_type = 'three_bit'
pointing_angle = -2*pi*40/360 % set array 40 degrees left
%pointing_angle = -2*pi*25/360 % set array "n" degrees left

% Radiation Pattern:
%[th,PHI,r] = meshgrid((0:5:360)*pi/180,(-90:2.5:90)*pi/180,1); % omni = 1
%[th,PHI,r] = meshgrid((0:10:360)*pi/180,(-90:5:90)*pi/180,1); % omni = 1
[th,PHI,r] = meshgrid((0:1:360)*pi/180,(-90:5:90)*pi/180,1); % omni = 1
r = antenna_pattern(antenna_type,PHI-(90*pi/180),th); % fix fi = vertical

```

```

wavesum = array_1D_shifted(quantity,pitch,shifter_type,pointing_angle,PHI-
(90*pi/180),th); % effect of summing antennas in-phase

subplot(2,2,1)

[X,Y,Z] = sph2cart(th,PHI,r);

hold off

surf(X,Y,Z)

title('Radiation Pattern of single element')

xlabel('X','FontSize',14);
ylabel('Y','FontSize',14);
zlabel('Z','FontSize',14);

subplot(2,2,2)

[X,Y,Z] = sph2cart(th,PHI,abs(wavesum));

```

```
surf(X,Y,Z)
title('Constructive/Destructive Interference')

subplot(2,2,3)
[X,Y,Z] = sph2cart(th,PHI,abs(r.*wavesum));
surfc(X,Y,Z)
title(sprintf('Combined Radiation Pattern of all %d elements at pitch %0.1g
lambda',quantity,pitch))

subplot(2,2,4)
polar(th,abs(r.*wavesum));
```

B. Antenna pattern

The function 'antenna_pattern', given an input of angles (in this case representing 360 degrees around and 180 degrees up and down) returns the radiation pattern of a single antenna element.

```
function X = antenna_pattern(antenna_type,theta,fi)
% EE299 Thesis - For an antenna (patch, dipole, etc) given angle,
% return gain in that direction

switch antenna_type
    case 'hertzian_dipole',
        % directivity of hertzian dipole is 1.5 or +1.76 dB
        X = 1.5 * sin(theta).^2;
    otherwise,
        X = 0;
        disp(antenna_type)
        disp(': antenna type not modeled')
end
```

C. Constructive and destructive interference

The function 'array_1D_shifted', returns the pattern of constructive and destructive interference from elements of a phased array. It is the radiation pattern that would occur if the antenna elements were spherical radiators (omni-directional).

```
function X = array_1D_shifted(quantity,pitch,shifter_type,pointing_angle,theta,fi)
% EE299 Thesis - For an antenna array given angle,
% Calls routine to look up shift and attenuation,
% sum effect of each antenna element
% return complex number representing constructive/destructive
% interference in given direction.
%(pattern of each antenna handled in a separate routine)

% theta ignored because it is vertical angle, and array assumed horizontal

if quantity < 1
    disp('quantity of antenna elements must be a positive integer')
% end
```

```

elseif rem(quantity,1) == 0
    % everything OK
    e_vector = 0;
    shift_and_magnitude = [0.0,0.0]; %[fi_prime, attenuation]
    shifts_and_magnitudes = zeros(quantity,2);
    %shifts_and_magnitudes

    for index = 0:1:quantity-1
        shift_and_magnitude = phase_shift(shifter_type,pointing_angle,pitch,index);
        e_vector = e_vector + shift_and_magnitude(2) *
exp(1j*(index*pitch*sin(fi)*2*pi-shift_and_magnitude(1))); % antenna element 'index'
        shifts_and_magnitudes(index+1,:) = shift_and_magnitude;
        % build array of shift at each antenna element
    end

```

```

X = e_vector;

shifts_and_magnitudes % display array

subplot(3,2,5)

plot(shifts_and_magnitudes)

else

    disp('Only integer quantity of antenna elements supported')

end

```

D. Phase shifter

The function 'phase_shift' computes the distance from a given antenna element to the wavefront in lambda and returns magnitude and phase for selected type of shifter.

```

function X = phase_shift(shifter_type,pointing_angle,pitch,index)

% EE299 Thesis -

% shift_and_magnitude = phase_shift(shifter_type,pointing,pitch,index);

```

```

switch shifter_type
    case 'ideal',
        shift = sin(pointing_angle)* pitch * index * 2*pi
        X = [shift,1.0];
    case 'three_bit', % 45 degree increments of coax
        shift = pi/4*round(sin(pointing_angle)* pitch * index * 2*pi/(pi/4));
        X = [shift,1.0];
    case 'YIG',
        idealshift = sin(pointing_angle)* pitch * index * 2*pi
        degrees = 360*idealshift/(2*pi)
        % range of possible inputs: beyond -180 degrees to +180 degrees

        index = round(rem(degrees,360)/10 + 18 - 0.5)+1
        % snap to nearest 10 degree increment in allowed range
        Sparm_arraysize = 36; % number of separate SParms

```

```

index = mod(index-1, Sparm_arraysize-1)+1;

    % wrap around beyond 360 degrees, but 1..36, not 0..35
MAG_51 = load('YIG_data\MAG.txt'); % Load SParm data
PHASE_51 = load('YIG_data\PHASE.txt');
freq_10G_index = 26; % position in SParm for nominal frequency

YIG_loss = -2.6; % dB loss at center of pass band
gain = 10^((MAG_51(freq_10G_index,index)-YIG_loss)/20)

    % convert dB to magnitude
%In previous line, gain of -2.6 dB was normalized to 0 dB.
%e.g. amplifier restores signal
shift = PHASE_51(freq_10G_index,index)/360 * 2*pi % return in radians
X = [shift,gain];
otherwise,
X = 0;

disp(shifter_type)

```

```

disp(': shifter type not modeled')

end

shift/(2*pi) * 360 % display degrees shift

```

E. Digital radio model and EVM calculation

The function 'FFT_test_filtered' is the top level routine used to simulate a QAM-16 digital radio and determine EVM when passing through a channel, for instance a phased array antenna system. When called with it produces plots of modulated IF data, constellations, errors seen at demodulation, and spectral content. It also returns EVM computed as the RSS of errors from each symbol recovered.

```

function X = FFT_test_filtered(beam_angle_degrees)

% EE299 Thesis - I-Q Modulate bit stream and transmit through channel
% filtered - Butterworth, YIG phase shifter (or other) filter transfer function
% recover I-Q symbols and compute EVM
% Also recover transmitted signal which is bandwidth limited but not
% filtered by the channel to determine increase in EVM due to phase shifter

```

```
% set up symbol rate

symbol_rate = 12.5e6 % 12.5 MHz symbol rate

points = 20; %

    per symbol 20 for good resolution to represent one cycle sine wave

Fs = symbol_rate * points; % sample rate 250 MHz

LO = 10e9 - symbol_rate;

%beam_angle = pi/6 % 30 degrees % phase shift only two values required
beam_angle = beam_angle_degrees/360 * 2* pi
%beam_angle = 40/360 * 2* pi % 40 degrees

numelements = 15

%numelements = 3

array_pitch = 1 % lambda or wavelengths
```

```
%shifter_type = 'ideal'

%shifter_type = 'three_bit'

%shifter_type = 'butterworth'

shifter_type = 'YIG'

%shifter_type = 'none'

plot_selection = 'debug'

plot_selection = 'transmitted'

plot_selection = 'modulated'

plot_selection = 'recovered'

% 16-QAM: 4 bits encoded in sixteen spots

bits_per_symbol = 4; % for hexadecimal

bits_per_half_symbol = bits_per_symbol/2;

value_per_half_symbol = 2^bits_per_half_symbol;
```

```

%bitstream_in = [0 1 2 3 4 5 6 7 8 9 10 11 12 13 14 15]' % for hexadecimal
bitstream_in = [0 15 4 11 8 7 12 3 13 2 14 1 10 5 6 9]' % bolt torqing pattern
%bitstream_in = [5 6 10 9 4 0 1 2 3 7 11 15 14 13 12 8]' % spiral out for
hexidecimal

symbols = 16;

% Split each symbol in half (low/high)
bithigh_in = floor(bitstream_in ./ value_per_half_symbol);
bitlow_in = mod(bitstream_in,value_per_half_symbol);

bithigh_centered = bithigh_in - (value_per_half_symbol/2 - 0.5);
bitlow_centered = bitlow_in - (value_per_half_symbol/2 - 0.5);

subplot(5,3,1)
plot(bitlow_centered,bithigh_centered,'o--')
title('Traversing the Constellation')

```

```
xlabel('I');  
ylabel('Q');  
  
subplot(5,3,4)  
stem(bitlow_centered)  
title('I')  
ylabel('I');  
  
subplot(5,3,7)  
stem(bithigh_centered)  
title('Q')  
ylabel('Q');  
  
% generate cos wave for I  
symbol_freq = 12.5; % MHz  
sample_freq = symbol_freq * points
```

```

% 80 ns/symbol, 20 points each, 4 ns per sample

t = 0:1/sample_freq:(points-1)/sample_freq; % time domain timebase
coswave = cos(2*pi*t*sample_freq/points + pi/4)';
hold off

subplot(5,3,2)
plot(t,coswave,'r')

sinwave = -sin(2*pi*t*sample_freq/points + pi/4)';
hold on

subplot(5,3,2)
plot(t,sinwave,'b')
title('cos & -sin for I & Q modulation')
hold off

% Piece-wise linear I & Q

```

```
I = [];  
Q = [];  
tt = [];  
for index = 0:1:symbols-1  
    I = [I; bitlow_centered(index+1) * coswave];  
    Q = [Q; bithigh_centered(index+1) * sinwave];  
    tt = [t, tt+points/sample_freq];  
end
```

```
subplot(5,3,5)
```

```
plot(tt,I')
```

```
title('cosine modulation of I')
```

```
subplot(5,3,8)
```

```
plot(tt,Q)
```

```
title('sine modulation of Q')
```

```

IQ_signal = I + Q;
subplot(5,3,3)
plot(tt,IQ_signal)
title('IQ modulation of bit stream')

% Done with time domain. Convert to frequency domain

IQ_signal_f = fft(IQ_signal,512); % 512 is a power of 2 > 320

% Implement a brick-wall digital filter to eliminate IF frequency
% components > 2x IF. Otherwise LO + IF and LO - IF overlap.
pass = 52; % pass first 50 frequency points un-altered = 25 MHz
halfpoints = length(IQ_signal_f)/2;
brick_wall = [ones(1,pass),zeros(1,halfpoints-pass), zeros(1,halfpoints-
pass),ones(1,pass)]]; % double-sided

```

```

% Filter IF signal

IQ_signal_f_transmitted = (IQ_signal_f .* brick_wall);

% Create array of frequencies for graphing/filtering purposes

NFFT = 2^nextpow2(length(IQ_signal));

% Next power of 2 from length of y e.g. 512 is a power of 2 > 320
f = Fs/2*linspace(0,1,NFFT/2+1); % out of 512 points, 257 = 512/2 + 1

%save 'debug_f.txt' f -ASCII % save in file for debug purposes

switch shifter_type
case 'butterworth',
    onesided_filter =
beamform_bandbutter_8th(f+LO,beam_angle,numelements,array_pitch);

```

```

case 'YIG',
    onesided_filter = beamform_YIG(f+LO,beam_angle,numelements,array_pitch);
otherwise,
    disp(shifter_type)
    disp(': shifter type not modeled; replace with ideal but BW limited
channel')
    % turn off channel degradation - revert to baseline
    onesided_filter = ones(1,NFFT/2+1);
end

doublesided_filter = [onesided_filter,
conj(fliplr(onesided_filter(2:length(onesided_filter)-1)))]';
    % actual orientation of frequency points in array
    doublesided_filter(NFFT/2+1) = 0; % even number of bits, first is DC. Kill the
one positive freq without corresponding negative freq

```

```

subplot(5,3,13)

degrade_phase = doublesided_filter; % Apply selected filter as phase shifter
degrade = degrade_phase; % a channel response by any other name

semilogy(abs(degrade)) % plot magnitude so complex isn't plotted real vs.
imaginary

title('Channel response')

IQ_signal_f_received = (IQ_signal_f_transmitted .* degrade); % linear rolloff

% The received signal has been shifted in time/phase
% shift back to synchronize for recovery of data

phase_correct = correct_delay(degrade_phase);

IQ_signal_f_corrected = IQ_signal_f_received .* phase_correct;

% Done with frequency domain. Convert back to time domain

```

```

IQ_signal_recovered = ifft(IQ_signal_f_corrected);

% As a baseline for comparison, also convert original signal without
degredation
IQ_signal_baseline = ifft(IQ_signal_f_transmitted);

% Now recover each symbol
% First, extract the timeslice with an IQ (QAM-16) encoding
bitlow_recovered = [];
bithigh_recovered = [];

bitlow_baseline = [];
bithigh_baseline = [];
for index = 0:1:symbols-1
    IQ_timeslice = IQ_signal_recovered(index*points +1:index*points +points);

```

```

        bitlow_recovered = [bitlow_recovered; 2*mean(IQ_timeslice .* coswave)]; %
"mean" serves to integrate over period

        bithigh_recovered = [bithigh_recovered; 2*mean(IQ_timeslice .* sinwave)];

        IQ_baseline = IQ_signal_baseline(index*points +1:index*points +points);
        bitlow_baseline = [bitlow_baseline; 2*mean(IQ_baseline .* coswave)];
        % "mean" serves to integrate over period
        bithigh_baseline = [bithigh_baseline; 2*mean(IQ_baseline .* sinwave)];

end

subplot(5,3,6)
stem(real(bitlow_recovered))
title('I recovered')
ylabel('I recovered');

subplot(5,3,9)

```

```

stem(real(bithigh_recovered))

title('Q recovered')

ylabel('Q recovered');

bitlow_centered
bitlow_recovered

subplot(5,3,10)
plot(real(bitlow_recovered),real(bithigh_recovered),'o--')
title('Recovered Constellation')
xlabel('I');
ylabel('Q');

% find error between original and recovered 'I' and 'Q'
bitlow_error = bitlow_recovered - bitlow_centered;
bithigh_error = bithigh_recovered - bithigh_centered;

```

```

% find error between baseline and recovered 'I' and 'Q'
bitlow_delta_error = bitlow_recovered - bitlow_baseline;
bithigh_delta_error = bithigh_recovered - bithigh_baseline;

subplot(5,3,11)
plot(real(bitlow_error),real(bithigh_error),'o--')
title('Constellation Error')
xlabel('I error');
ylabel('Q error');

% Compute RMS error
RMS_error = (mean([bitlow_error.^2; bithigh_error.^2]))^0.5
EVM_percent = RMS_error/0.5 * 100

RMS_delta_error = (mean([bitlow_delta_error.^2; bithigh_delta_error.^2]))^0.5

```

```

EVM_delta_percent = RMS_delta_error/0.5 * 100

X = EVM_delta_percent; % Give as return from this function

% study behavior of fft on coswave

coswave_f = fft(coswave); % frequency domain of coswave
sinwave_f = fft(sinwave); % frequency domain of sinwave

% Construct a frequency axis

fftpoints = 1:1:512;

subplot(5,3,12)

hold off

plot(fftpoints,abs(IQ_signal_f),'r')

hold on

plot(fftpoints,abs(IQ_signal_f_transmitted),'b')

```

```
hold off

title('IQ signal f frequency domain')

xlabel('frequency (Mhz)');

ylabel('|signal|');

coswave_recovered = ifft(coswave_f);
sinwave_recovered = ifft(sinwave_f);

hold off

subplot(5,3,14)

plot(t,coswave_recovered,'r')

hold on

subplot(5,3,14)

plot(t,sinwave_recovered,'b')

title('recovered cos & -sin for I & Q modulation')
```

```
hold off

% overwrite with different plot
subplot(5,3,14)
plot(real(bitlow_delta_error),real(bithigh_delta_error),'o--')
title('delta Constellation Error')
xlabel('I error');
ylabel('Q error');

% plot error
hold off
subplot(5,3,15)
plot(t,coswave_recovered - coswave,'r')

hold on
subplot(5,3,15)
```

```

plot(t,sinwave_recovered - sinwave,'b')
title('error in recovered cos & -sin')
hold off

% overwrite with different plot
hold off
plot(fftpoints,angle(degrade_phase),'b')
hold on
plot(fftpoints,angle(phase_correct),'r')
hold off
title('filter phase')
xlabel('frequency (Mhz)');
ylabel('phase of filter');

```

F. Idealized Butterworth beam former

The function ‘beamform_bandbutter_8th’ returns the S-parameters (normalized to 1.0 magnitude at center frequency) for a phased array antenna system, with an idealized Butterworth filter serving as phase shifter.

```

function X = beamform_bandbutter_8th(f,beam_angle,numelements,pitch)

% model beamforming using 8th order bandpass filter as phase-shifter
% called with a set of frequency points and beam angle, returns S21 parameters

% Works by summing delayed results from phaseshift_bandbutter_8th

formedbeam = zeros(1,length(f));

for element = 1:1:numelements

    phase_angle = rem((sin(beam_angle) * (element-1) * pitch * 2*pi)+pi, 2*pi)-
pi

    delay = exp(-1j.*phase_angle*f./f(26));
    angle(delay(26))
    abs(delay(26))

    phaseshifted_wavefront = phaseshift_bandbutter_8th(f,phase_angle);
    angle(phaseshifted_wavefront(26))

    delayed_wavefront = -delay .* phaseshifted_wavefront;

```

```

    angle(delayed_wavefront(26))

    formedbeam = formedbeam + delayed_wavefront;

end

net_multiple = abs(formedbeam(26)) % errors in picking phase - re-scale output
amplitude

formedbeam = formedbeam ./ net_multiple;

X = formedbeam; % return S21 parameter

```

G. Idealized Butterworth phase shifter

The function ‘phaseshift_bandbutter_8th’ estimates the center frequency a Butterworth band-pass filter should be tuned to in order to produce the desired phase shift and returns S-parameters.

```

function X = phaseshift_bandbutter_8th(f, angle)

% model beamforming using 8th order bandpass filter as phase-shifter
% called with a set of frequency points and beam angle, returns S21 parameters

```

```

% with settings wl = 1.5*w; wh = 0.667*w;

% +209 degrees at 4.3e10 rad/sec

% 0 degrees at 6.28e10 rad/sec

% -200 degrees at 9.06e10 rad/sec

% find two slopes, one for positive phase shift, the other negative phase shift

plus209freq = 4.3e10/(2*pi);
plus0freq = 6.28e10/(2*pi);
minus200freq = 9.06e10/(2*pi);

plus_degrees_per_hz = 209 / (plus209freq - plus0freq);
plus_radians_per_hz = 2*pi*plus_degrees_per_hz/360;
plus_hz_per_radian = 1/plus_radians_per_hz;

minus_degrees_per_hz = (209 - (-200))/(plus209freq - minus200freq);

```

```

minus_radians_per_hz = 2*pi*minus_degrees_per_hz/360;
minus_hz_per_radian = 1/minus_radians_per_hz;

fnom = 10e9; % 10 GHz nominal frequency for no phase shift
angle;

if angle >= 0
    offnom = fnom + angle * plus_hz_per_radian;
else
    offnom = fnom + angle * minus_hz_per_radian;
end

w = 2*pi*offnom; % radians
% following values for broad passband
wl = 1.5*w; % cutoff by lowpass filter; high frequency cutoff of bandpass
wh = 0.667*w; % cutoff by highpass filter; low frequency cutoff of bandpass

```

```

glow = tf([1],[1/wl^8 5.1258/wl^7 13.13695771/wl^6 21.84596388/wl^5 25.6881355/wl^4
21.84596388/wl^3 13.13695771/wl^2 5.1258/wl 1]);

ghigh = tf([1/wh^8 0 0 0 0 0 0 0 0],[1/wh^8 5.1258/wh^7 13.13695771/wh^6
21.84596388/wh^5 25.6881355/wh^4 21.84596388/wh^3 13.13695771/wh^2 5.1258/wh 1]);

g = glow * ghigh;

%bode(g)

[MAG,PHASE] = bode(g,f*2*pi);

SPARM = MAG(:, :).*cos(2*pi/360*PHASE(:, :)) + 1i *
MAG(:, :).*sin(2*pi/360*PHASE(:, :));

X = SPARM; % return S21 parameter

```

H. Recovery synchronization

The function ‘correct_delay’ determines the phase shift introduced in the center of the IF frequency by the S-parameters representing the sum of the contribution of all antenna elements (each of which is at a different distance from the target). In an

actual system this would be performed by adjusting a phase-locked loop or by analyzing the sampled IF waveform, but for purposes of this model it is simply determined from the calculated channel response. This routine performs a second function as well. For a phased array antenna the function which is actually desired from a phase shifter is to delay the signal to each antenna element, irrespective of frequency, such that all reach the target destination at the same time. The phase shifter provides the necessary relative shift between antenna elements to achieve constructive interference. However, by heavily filtering the signals, the analog phase shifter introduces a frequency-dependent phase shift is introduced into the signal that is delivered to the destination (or received.) This can be compensated for in the digital realm by pre-compensating transmitted signals or post-compensating received signals based on characterized behavior. The function 'correct_delay' performs this with a simple linear predicted response, the slope of the phase shift between the lowest frequency component in the signal and the center of the IF frequency. The phase error which remains is due to non-linearity of the YIG phase shifter. While this code could have been written with a calibration constant for the slope, it was instead made adaptive so as to work with any selected phase shifter (e.g. the higher order ideal Butterworth filter.)

```
function X = correct_delay(filter_response)
% EE299 Thesis - given filter_response (a phase shifter)
%     create an inverse phase filter to correct phase response at IF
%     Presumption is the delay needs to be corrected.  But, rather
```

```

%      than introducing the time component into a frequency domain model,
%      each frequency is just phase shifted.  For signals which
%      undergo more than 360 degrees shift this is not correct; antenna
%      elements more than one IF cycle from the wavefront will carry
%      modulated data from a different symbol

NFFT = length(filter_response);

IF_index = 26; % The IF frequency is represented by element 26 in array

% unwind phase shift from filter
shift_IF = angle(filter_response(IF_index))

% phase shift at location of 1/2 IF
shift_min_f = angle(filter_response(2))

% phase shift at lowest frequency component
if (shift_IF < 0) && (shift_min_f > 0)
    shift_IF = shift_IF + 2*pi;

```

```

        % wrapped around because > +1 pi; represent as +1.x pi

end

shift_slope = (shift_IF-shift_min_f)/(IF_index-1);

points_slope = 2:1:NFFT/2;

linear_slope = exp(- 1i .* (shift_IF + (points_slope - IF_index) .*
(shift_slope)))';

linear_correct = [1; linear_slope];

max_f_point = NFFT/2; % Half of points represent positive frequencies, the
other half negative frequencies

phase_correct = zeros(1,NFFT);

phase_correct(1:max_f_point) = linear_correct;

% linear slope for positive frequencies

phase_correct(NFFT-max_f_point+2:NFFT) =
conj(flipud((linear_correct(2:max_f_point))));

```

```
% reverse slope for negative frequencies
```

```
phase_correct = phase_correct';
```

```
X = phase_correct;
```

1. YIG beam former

The function 'beamform_YIG' returns the S-parameters (normalized to 1.0 magnitude at center frequency) for a phased array antenna system using measured YIG bandpass filter S-paramters.

```
function X = beamform_YIG(f,beam_angle,numelements,pitch)
```

```
% model beamforming using measured YIG SParms
```

```
% called with a set of frequency points and beam angle, returns S21 parameters
```

```
% representing channel response in direction of beam
```

```
% Instead of starting at zero degrees, start at +60 degrees so very small
```

```
% angles can be obtained with the +60 to +180 angles for which
```

```
% the measured YIG filter was within its -3dB passband
```

```
first_element_angle = 60; % degrees
```

```

rad_start = first_element_angle/360 * 2 * pi; %radians

% Works by summing delayed results from phaseshift_YIG

formedbeam = zeros(1,length(f));

for element = 1:1:numelements
    phase_angle = rem((sin(beam_angle) * (element-1) * pitch)+pi + rad_start,
2*pi)-pi
    delay = exp(-1j.*phase_angle*f./f(26));

    % Compute phase shift from delay between antenna element and wavefront

abs_delay = abs(delay(26)) % debug
degrees_angle_delay = angle(delay(26)) *360/(2*pi) % debug

phaseshifted_wavefront = phaseshift_YIG(f,phase_angle);
abs_phaseshift = abs(phaseshifted_wavefront(26)) % debug

```

```

degrees_angle_phaseshift = angle(phaseshifted_wavefront(26)) *360/(2*pi) %
debug

delayed_wavefront = -delay .* phaseshifted_wavefront;

    % Propagation delay shifts phase of each frequency

abs_delayed_wavefront = abs(delayed_wavefront(26)) % debug

degrees_angle_delayed_wavefront = angle(delayed_wavefront(26)) *360/(2*pi) %
debug

formedbeam = formedbeam + delayed_wavefront;

end

% Automatic Gain Control should be processed in receiver/de-modulator
% But to keep it simple, channel gain is normalized to 1.0 at center
% frequency:

net_multiple = abs(formedbeam(26)) % re-scale output amplitude for 1.0 output

```

```
formedbeam = formedbeam ./ net_multiple;
```

```
X = formedbeam; % return S21 parameter
```

J. YIG phase shifter

The function 'phaseshift_YIG' looks up an S-parameter file with phase shift closest to the desired amount. The files provide 10 degree increments, so the result is within +/- 5 degrees.

```
function X = phaseshift_YIG(f, angle)
```

```
% beamforming using measured SParms from YIG filter as phase-shifter
```

```
% called with a set of frequency points and beam angle, returns S21 parameters
```

```
fnom = 10e9; % 10 GHz nominal frequency for no phase shift
```

```
angle;
```

```
degrees = 360*angle/(2*pi) % range of possible inputs: -180 degrees to +180 degrees
```

```
index = round(rem(degrees,360)/10 + 18 - 0.5)+1 % snap to nearest 10 degree
```

```
increment
```

```

% load SParms from file

MAG_51 = load('YIG_data\MAG.txt');
PHASE_51 = load('YIG_data\PHASE.txt');

zip = -1e+5; % pad with values near zero outside 25MHz bandwidth

dB_MAG = [zip*ones(1,1),MAG_51(:,index)',zip*ones(1,257-51-1)];
% out of 512 points, 257 = 512/2 + 1
PHASE = [zeros(1,1),PHASE_51(:,index)',zeros(1,257-51-1)];
% out of 512 points, 257 = 512/2 + 1

% measured S-parm file was logarithmic; change to linear before
% creating complex values
MAG = 10.^(dB_MAG./20); % MAGDB = 20*log10(MAG);

```

```

SPARM = MAG(:, :).*cos(2*pi/360*PHASE(:, :)) + 1i *
MAG(:, :).*sin(2*pi/360*PHASE(:, :));
X = SPARM; % return S21 parameter

```

K. Swept beam angle

The function 'EVM_test' invokes FFT_test_filtered() with beam angles from 0° to +85° and produces a graph of EVM vs. beam angle.

```

function X = EVM_test
% Sweep beam angle, report EVM

angle = []
delta_EVM = []
for angle_degrees = 0:5:85;
    angle = [angle, angle_degrees];
    delta_EVM = [delta_EVM, FFT_test_filtered(angle_degrees)]

```

```

end

subplot(5,3,13)
plot(angle,abs(delta_EVM))
title('delta EVM due to YIG phase shifter')
    xlabel('beam angle (degrees)');
    ylabel('delta EVM');

```

L. Read S-parameter files and store in array

The function 'load_test' reads 36 S-parameter files (that have had the header information removed for easier parsing) and extracts the frequency, S21 magnitude, and S21 phase information. It stores these in three files for use by the other programs and plots a family of curves for magnitude and phase.

```

function X = load_test
% Loading s-paramter files, save arrays of frequency, S21_mag, S21_phase

```

```

% case for plotting.  plots 4 & 6 final

plot_selection = 'debug'
plot_selection = 'final'

% format:

% !S2P File: Measurements: S11, S21, S12, S22:

% # Hz S   dB   R 50

% freq S11_mag S11_degrees S21_mag S21_degrees S12_mag S12_degrees S22_mag
S22_degrees

datafiles =
['YIG_data\yigm_180.txt'; 'YIG_data\yigm_170.txt'; 'YIG_data\yigm_160.txt'];

datafiles =
[datafiles; 'YIG_data\yigm_150.txt'; 'YIG_data\yigm_140.txt'; 'YIG_data\yigm_130.txt'];

datafiles =
[datafiles; 'YIG_data\yigm_120.txt'; 'YIG_data\yigm_110.txt'; 'YIG_data\yigm_100.txt'];

```

```
datafiles = [datafiles;'YIG_data\yigm_90.txt '; 'YIG_data\yigm_80.txt  
';'YIG_data\yigm_70.txt '];  
datafiles = [datafiles;'YIG_data\yigm_60.txt '; 'YIG_data\yigm_50.txt  
';'YIG_data\yigm_40.txt '];  
datafiles = [datafiles;'YIG_data\yigm_30.txt '; 'YIG_data\yigm_20.txt  
';'YIG_data\yigm_10.txt '];  
datafiles = [datafiles;'YIG_data\yigp_0.txt  '; 'YIG_data\yigp_10.txt  
';'YIG_data\yigp_20.txt '];  
datafiles = [datafiles;'YIG_data\yigp_30.txt '; 'YIG_data\yigp_40.txt  
';'YIG_data\yigp_50.txt '];  
datafiles = [datafiles;'YIG_data\yigp_60.txt '; 'YIG_data\yigp_70.txt  
';'YIG_data\yigp_80.txt '];  
datafiles = [datafiles;'YIG_data\yigp_90.txt  
';'YIG_data\yigp_100.txt'; 'YIG_data\yigp_110.txt'];  
datafiles =  
[datafiles;'YIG_data\yigp_120.txt'; 'YIG_data\yigp_130.txt'; 'YIG_data\yigp_140.txt'];
```

```
datafiles =  
[datafiles; 'YIG_data\yigp_150.txt'; 'YIG_data\yigp_160.txt'; 'YIG_data\yigp_170.txt'];  
  
datafiles(10,:) =  
fpoints = 51  
fpoint_10G = 26;  
num_sparms = 36  
hold on  
  
MAG = zeros(fpoints, num_sparms);  
PHASE = zeros(fpoints, num_sparms);  
  
for fileindex = 1:1:num_sparms;  
    yig_sparm = load(datafiles(fileindex,:));  
  
    f = yig_sparm(:,1);
```

```
MAG(:,fileindex) = yig_sparm(:,4);  
PHASE(:,fileindex) = yig_sparm(:,5);  
  
switch lower(plot_selection)  
    case 'debug'  
        subplot(3,2,1)  
    case 'final'  
        subplot(2,1,1) % will be overwritten  
    otherwise  
        subplot(3,2,1)  
end  
  
hold on  
  
plot(f,MAG(:,fileindex))  
  
title('Gain: Good except for some ripple')
```

```
switch lower(plot_selection)
    case 'debug'
        subplot(3,2,3)
    case 'final'
        subplot(2,1,1) % will be overwritten
    otherwise
        subplot(3,2,3)
end

hold on

plot(f,PHASE(:,fileindex))

title('Phase: Good except for slight ripple')

end
```

```
freq_plotted = f(fpoint_10G)
switch lower(plot_selection)
    case 'debug'
        subplot(3,2,5)
    case 'final'
        subplot(2,1,1) % will be overwritten
    otherwise
        subplot(3,2,5)
end
plot(MAG(fpoint_10G,:))
title('Response at 10 GHz as a function of selected phase shift')

MAG(:,fpoint_10G)

max(MAG) '
```

```

picked_index = 9 % an SParm with good representative flatness
picked_phase = PHASE(fpoint_10G,picked_index)
    % What nominal 10GHz phase for that SParm
switch lower(plot_selection)
    case 'debug'
        subplot(3,2,2)
    case 'final'
        subplot(2,1,1) % will be overwritten
    otherwise
        subplot(3,2,2)
end
hold off
plot(f,MAG(:,picked_index))

title('Pick a Gain, any gain (e.g. index 9, -100 degrees)')

```

```
switch lower(plot_selection)
    case 'debug'
        subplot(3,2,4)
    case 'final'
        subplot(2,1,2) % will be overwritten
    otherwise
        subplot(3,2,4)
end

hold off

plot(f,PHASE(:,picked_index))

title('Phase of a Gain, any gain')

save 'YIG_data\MAG.txt' MAG -ASCII
save 'YIG_data\PHASE.txt' PHASE -ASCII
save 'YIG_data\f.txt' f -ASCII
```

```
switch lower(plot_selection)
    case 'debug'
        subplot(3,2,6)
    case 'final'
        subplot(2,1,2)
    otherwise
        subplot(3,2,6)
end

hold off

plot(f, PHASE(:, :))
title('Phase: Good except for slight ripple')
    xlabel('frequency (Hz)');
    ylabel('phase (degrees)');

% overwrite earlier plot:
```

```
switch lower(plot_selection)
    case 'debug'
        subplot(3,2,4)
    case 'final'
        subplot(2,1,1)
    otherwise
        subplot(3,2,4)
end
plot(f,MAG(:, :))
title('Gain: Good except for some ripple')
    xlabel('frequency (Hz)');
    ylabel('gain (dB)');
```

M. Read and plot filter S-parameter across entire passband

The function 'load_bandpass' reads 5 S-parameter files (that have had the header information removed for easier parsing) and plots the data across a 200 MHz wide frequency range, showing the YIG filter's 50 MHz -3 dB bandwidth centered about the 10 GHz carrier frequency, then shifted up and down to provide +/- 180° phase shift relative to the centered one.

```
function X = load_bandpass
% Loading s-paramter files showing bandpass, 200 MHz bw around 10 GHz
% save arrays of frequency, S21_mag, S21_phase

% case for plotting. 4 & 6 final
plot_selection = 'debug'
plot_selection = 'final'

% Input format:
% !S2P File: Measurements: S11, S21, S12, S22:
% # Hz S dB R 50
```

```

% freq S11_mag S11_degrees S21_mag S21_degrees S12_mag S12_degrees S22_mag
S22_degrees

%filename strings padded with spaces to be same length
datafiles = ['YIG_data\yig_10g_left.txt           '; 'YIG_data\yig_10g_left_center.txt
'; 'YIG_data\yig_10g_center.txt           '];
datafiles =
[datafiles; 'YIG_data\yig_10g_right_center.txt'; 'YIG_data\yig_10g_right.txt           '];

datafiles(3,:)

fpoints = 51
fpoint_10G = 26;
num_sparms = 5
hold on

MAG = zeros(fpoints, num_sparms);

```

```
PHASE = zeros(fpoints, num_sparms);

for fileindex = 1:1:num_sparms;
    yig_sparm = load(datafiles(fileindex,:));

    f = yig_sparm(:,1);

    MAG(:,fileindex) = yig_sparm(:,4);
    PHASE(:,fileindex) = yig_sparm(:,5);

switch lower(plot_selection)
    case 'debug'
        subplot(3,2,1)
    case 'final'
        subplot(2,1,1) % will be overwritten
    otherwise
```

```
        subplot(3,2,1)
end
    hold on
    plot(f,MAG(:,fileindex))

    title('Gain: Good except for some ripple')

switch lower(plot_selection)
    case 'debug'
        subplot(3,2,3)
    case 'final'
        subplot(2,1,1) % will be overwritten
    otherwise
        subplot(3,2,3)
end
    hold on
```

```
plot(f, PHASE(:, fileindex))

title('Phase: Good except for slight ripple')

end

freq_plotted = f(fpoint_10G)
switch lower(plot_selection)
    case 'debug'
        subplot(3,2,5)
    case 'final'
        subplot(2,1,1) % will be overwritten
    otherwise
        subplot(3,2,5)
end

plot(MAG(fpoint_10G, :))
```

```

title('Response at 10 GHz as a function of selected phase shift')

MAG(fpoint_10G,:)

max(MAG) '

picked_index = 3 % an SParm with good representative flatness
picked_phase = PHASE(fpoint_10G,picked_index)
    % What nominal 10GHz phase for that SParm
switch lower(plot_selection)
    case 'debug'
        subplot(3,2,2)
    case 'final'
        subplot(2,1,1) % will be overwritten
    otherwise
        subplot(3,2,2)

```

```
end

hold off

plot(f,MAG(:,picked_index))

title('Pick a Gain, any gain (e.g. index 9, -100 degrees)')

switch lower(plot_selection)
    case 'debug'
        subplot(3,2,4)
    case 'final'
        subplot(2,1,2) % will be overwritten
    otherwise
        subplot(3,2,4)
end

hold off

plot(f,PHASE(:,picked_index))
```

```
title('Phase of a Gain, any gain')

save 'YIG_data\bandpass_MAG.txt' MAG -ASCII
save 'YIG_data\bandpass_PHASE.txt' PHASE -ASCII
save 'YIG_data\bandpass_f.txt' f -ASCII

switch lower(plot_selection)
    case 'debug'
        subplot(3,2,6)
    case 'final'
        subplot(2,1,2)
    otherwise
        subplot(3,2,6)
end

hold off
```

```

plot(f, PHASE(:, :))
title('Phase: Good except for slight ripple')
    xlabel('frequency (Hz)');
    ylabel('phase (degrees)');

% overwrite earlier plot:
switch lower(plot_selection)
    case 'debug'
        subplot(3,2,4)
    case 'final'
        subplot(2,1,1)
    otherwise
        subplot(3,2,4)
end

plot(f, MAG(:, :))
title('Gain: Good except for some ripple')

```

```
xlabel('frequency (Hz)');
```

```
ylabel('gain (dB)');
```

DATA FILES

This section contains representative samples of data.

A. YIG S-parameter

The following listing is a raw S-parameter file obtained from the YIG filter. Only the S21 parameter was used. The columns of the table are:

Freq, S11mag, S11phase, S21mag, S21phase, S12mag, S12phase, S22mag, S22phase,

Units for frequency: Hz, for magnitude: dB, for phase: degrees

```
!Agilent Technologies,E8364B,MY43040657,A.07.50.26
```

```
!Agilent E8364B: A.07.50.26
```

```
!Date: Saturday, March 05, 2011 13:59:16
```

```
!Correction: S11(Full 2 Port(1,2))
```

```
!S21(Full 2 Port(1,2))
```

```
!S12(Full 2 Port(1,2))
```

```
!S22(Full 2 Port(1,2))
```

!S2P File: Measurements: S11, S21, S12, S22:

Hz S dB R 50

9987790000 -2.137880e+001 1.084778e+002 -3.282870e+000 -4.311288e+001 -2.763350e+000

1.564315e+002 -1.843445e+001 1.686666e+002

9988278200 -2.107807e+001 1.085379e+002 -3.224191e+000 -4.595632e+001 -2.754102e+000

1.540602e+002 -1.796189e+001 1.709051e+002

9988766400 -2.083906e+001 1.085832e+002 -3.185504e+000 -4.863684e+001 -2.750721e+000

1.517571e+002 -1.748332e+001 1.719006e+002

9989254600 -2.069933e+001 1.087286e+002 -3.162029e+000 -5.113791e+001 -2.754327e+000

1.495369e+002 -1.700962e+001 1.720140e+002

9989742800 -2.053877e+001 1.089825e+002 -3.137861e+000 -5.349100e+001 -2.759594e+000

1.474141e+002 -1.660704e+001 1.712774e+002

9990231000 -2.034829e+001 1.090699e+002 -3.106183e+000 -5.573370e+001 -2.754377e+000

1.453271e+002 -1.631416e+001 1.700258e+002

9990719200 -2.011570e+001 1.087308e+002 -3.066542e+000 -5.796666e+001 -2.749722e+000

1.432760e+002 -1.609472e+001 1.686198e+002

9991207400 -1.994893e+001 1.078469e+002 -3.024184e+000 -6.022639e+001 -2.737374e+000
1.412199e+002 -1.593337e+001 1.670730e+002
9991695600 -1.980682e+001 1.065774e+002 -2.983601e+000 -6.247739e+001 -2.725991e+000
1.391652e+002 -1.583575e+001 1.655588e+002
9992183800 -1.969462e+001 1.050963e+002 -2.944382e+000 -6.474444e+001 -2.712220e+000
1.370897e+002 -1.577852e+001 1.640467e+002
9992672000 -1.965395e+001 1.033021e+002 -2.909216e+000 -6.702081e+001 -2.700158e+000
1.350273e+002 -1.575069e+001 1.625626e+002
9993160200 -1.968834e+001 1.015403e+002 -2.884315e+000 -6.931145e+001 -2.692257e+000
1.329182e+002 -1.575141e+001 1.610822e+002
9993648400 -1.974854e+001 9.980165e+001 -2.860499e+000 -7.157809e+001 -2.683906e+000
1.308478e+002 -1.577917e+001 1.596426e+002
9994136600 -1.983236e+001 9.816721e+001 -2.844693e+000 -7.383586e+001 -2.678052e+000
1.287735e+002 -1.581485e+001 1.580027e+002
9994624800 -1.994011e+001 9.663168e+001 -2.828729e+000 -7.602969e+001 -2.672827e+000
1.267350e+002 -1.588360e+001 1.562048e+002

9995113000 -2.004565e+001 9.506959e+001 -2.809125e+000 -7.824432e+001 -2.665832e+000
1.246518e+002 -1.601442e+001 1.543782e+002
9995601200 -2.019018e+001 9.352750e+001 -2.792871e+000 -8.047071e+001 -2.660445e+000
1.225674e+002 -1.617921e+001 1.525700e+002
9996089400 -2.035042e+001 9.198404e+001 -2.780307e+000 -8.270508e+001 -2.657848e+000
1.204755e+002 -1.638533e+001 1.507281e+002
9996577600 -2.055563e+001 9.075974e+001 -2.772460e+000 -8.492853e+001 -2.659364e+000
1.183533e+002 -1.660760e+001 1.489901e+002
9997065800 -2.074644e+001 8.983188e+001 -2.770678e+000 -8.713496e+001 -2.662204e+000
1.162718e+002 -1.684722e+001 1.471181e+002
9997554000 -2.092867e+001 8.915650e+001 -2.771702e+000 -8.930810e+001 -2.672327e+000
1.141860e+002 -1.710550e+001 1.451243e+002
9998042200 -2.103799e+001 8.868250e+001 -2.771138e+000 -9.145021e+001 -2.679645e+000
1.121289e+002 -1.740034e+001 1.428768e+002
9998530400 -2.112583e+001 8.817115e+001 -2.771347e+000 -9.356522e+001 -2.692712e+000
1.100868e+002 -1.773140e+001 1.403258e+002

9999018600 -2.116773e+001 8.765734e+001 -2.766345e+000 -9.568748e+001 -2.697983e+000
1.080513e+002 -1.813193e+001 1.375023e+002
9999506800 -2.116063e+001 8.689763e+001 -2.758945e+000 -9.777220e+001 -2.705790e+000
1.060101e+002 -1.859782e+001 1.343736e+002
9999995000 -2.114283e+001 8.606619e+001 -2.746349e+000 -9.980790e+001 -2.710562e+000
1.040143e+002 -1.911402e+001 1.310208e+002
10000483200 -2.111561e+001 8.506052e+001 -2.744264e+000 -1.020508e+002 -
2.725312e+000 1.018804e+002 -1.977319e+001 1.271158e+002
10000971400 -2.107468e+001 8.397672e+001 -2.734247e+000 -1.041985e+002 -
2.739695e+000 9.980454e+001 -2.050254e+001 1.230231e+002
10001459600 -2.103452e+001 8.277034e+001 -2.730330e+000 -1.063288e+002 -
2.757500e+000 9.774010e+001 -2.132902e+001 1.183027e+002
10001947800 -2.093999e+001 8.140791e+001 -2.720279e+000 -1.084992e+002 -
2.780494e+000 9.570447e+001 -2.225273e+001 1.128561e+002
10002436000 -2.085586e+001 7.990858e+001 -2.713622e+000 -1.106523e+002 -
2.807003e+000 9.370177e+001 -2.325502e+001 1.066197e+002

10002924200 -2.079096e+001 7.833344e+001 -2.702918e+000 -1.128227e+002 -
2.828071e+000 9.174594e+001 -2.432952e+001 9.883500e+001
10003412400 -2.070745e+001 7.646339e+001 -2.696863e+000 -1.150069e+002 -
2.845854e+000 8.986693e+001 -2.535269e+001 8.931226e+001
10003900600 -2.066497e+001 7.464382e+001 -2.676817e+000 -1.172031e+002 -
2.849108e+000 8.800835e+001 -2.620315e+001 7.726466e+001
10004388800 -2.067926e+001 7.289611e+001 -2.657427e+000 -1.194526e+002 -
2.839993e+000 8.610764e+001 -2.671053e+001 6.268938e+001
10004877000 -2.072787e+001 7.138839e+001 -2.642978e+000 -1.217686e+002 -
2.815195e+000 8.413612e+001 -2.665287e+001 4.601712e+001
10005365200 -2.078213e+001 7.037801e+001 -2.630318e+000 -1.241547e+002 -
2.792984e+000 8.203975e+001 -2.601735e+001 3.023911e+001
10005853400 -2.079287e+001 7.007783e+001 -2.622703e+000 -1.265760e+002 -
2.773475e+000 7.986189e+001 -2.491346e+001 1.629474e+001
10006341600 -2.075246e+001 7.015565e+001 -2.625163e+000 -1.290096e+002 -
2.765133e+000 7.760550e+001 -2.363310e+001 5.151568e+000

10006829800 -2.060288e+001 7.052211e+001 -2.630555e+000 -1.314872e+002 -
2.766804e+000 7.531703e+001 -2.228909e+001 -3.724095e+000
10007318000 -2.037527e+001 7.085364e+001 -2.644888e+000 -1.339624e+002 -
2.772380e+000 7.307545e+001 -2.097273e+001 -1.070551e+001
10007806200 -2.007879e+001 7.095077e+001 -2.663668e+000 -1.364706e+002 -
2.779284e+000 7.082498e+001 -1.967251e+001 -1.641056e+001
10008294400 -1.974001e+001 7.090582e+001 -2.688922e+000 -1.390145e+002 -
2.779178e+000 6.853879e+001 -1.846660e+001 -2.159624e+001
10008782600 -1.936754e+001 7.095555e+001 -2.720986e+000 -1.415580e+002 -
2.784551e+000 6.615653e+001 -1.735441e+001 -2.625483e+001
10009270800 -1.894173e+001 7.089249e+001 -2.766097e+000 -1.441190e+002 -
2.795650e+000 6.370614e+001 -1.634562e+001 -3.053660e+001
10009759000 -1.846123e+001 7.064160e+001 -2.815098e+000 -1.466649e+002 -
2.824914e+000 6.120231e+001 -1.543145e+001 -3.452660e+001
10010247200 -1.794053e+001 7.026072e+001 -2.875136e+000 -1.492379e+002 -
2.859888e+000 5.867234e+001 -1.460460e+001 -3.815626e+001

10010735400 -1.737218e+001 6.957539e+001 -2.938832e+000 -1.517634e+002 -
2.910384e+000 5.618197e+001 -1.384959e+001 -4.145423e+001
10011223600 -1.678653e+001 6.852161e+001 -3.013395e+000 -1.542745e+002 -
2.967156e+000 5.368087e+001 -1.316378e+001 -4.448265e+001
10011711800 -1.619380e+001 6.712275e+001 -3.090793e+000 -1.567698e+002 -
3.034881e+000 5.120901e+001 -1.252610e+001 -4.727071e+001
10012200000 -1.560187e+001 6.551572e+001 -3.173349e+000 -1.592468e+002 -
3.107358e+000 4.876628e+001 -1.193639e+001 -4.990760e+001

REFERENCES

- [1] Microlambda Wireless, available on web site <http://www.microlambdawireless.com>
- [2] V. E. Demidov, B. A. Kalinikos, S. F. Karmanenko, A. A. Semenov, P. Edenhofer, "Electrical tuning of dispersion characteristics of surface electromagnetic-spin waves propagating in ferrite-ferroelectric layered structures," *IEEE Transactions on Microwave Theory and Techniques*, vol. 51, no. 10, pp. 2090-2096, October 2003.
- [3] H. How, P. Shi, C. Vittoria, E. Hokanson, M. H. Champion, L. C. Kempel, K. D. Trott, "Steerable phased array antennas using single-crystal YIG phase shifters – theory and experiments," *IEEE Transactions on Microwave Theory and Techniques*, vol. 48, no. 9, pp. 1544-1549, September 2000.
- [4] A. S. Tatarenko, G. Srinivasan, M. I. Bichurin, "Electrically-tunable microwave phase shifter based on ferrite-piezoelectric layered structure," 18th Intl. Crimean Conference "Microwave & Telecommunication Technology"/IEEE, CFP08788, pp. 507, 508, September 2008.
- [5] B. Foster, I. Gonin, T. Khabiboulline, A. Makarov, N. Solyak, I. Terechkine, and D. Wildman, "High power phase shifter," *Proceedings of 2005 Particle Accelerator Conference, Knoxville/IEEE 0-7803-8859-3/05, 0-7803-8859-3/05*, pp. 3123-3125, 2005.
- [6] M. Cohen, "An alignment technique for multiple ball YIG bandpass filters operating over multi-octave frequency bands," *Microwave Symposium Digest, IEEE-MTT-S International*, pp. 33-36, 1978.
- [7] G. Bryant, *Principles of Microwave Measurements*. Stevenage, United Kingdom: Peter Peregrinus Ltd., 1993.
- [8] F. Ulaby, *Electromagnetics for Engineers*. Upper Saddle River, NJ: Pearson Prentice Hall, 2005.